Table I. *MiR-15a expression and clinicopathological factors*

	Low expression (n=124)		High expression (n=106)		
Factors	Number	%	Number	%	*p*-Value
Age (mean±SD*1)	56±12		54±11		0.053
Estrogen receptor					0.90
Positive	66	53	55	52	
Negative	58	47	50	48	
Progestrone receptor					0.44
Positive	66	54	51	49	
Negative	57	46	54	51	
HER2					0.40
Positive	32	28	35	33	
Negative	82	72	70	67	
T factors					0.33
Tis-I	78	63	60	57	
T2-4	46	37	46	43	
Lymph node metastasis					0.59
Absent	71	57	58	55	
Present	53	43	48	45	
Nuclear Grade					0.30
1-2	81	69	62	62	
3	37	31	38	38	
Lymphatic invasion					0.62
Absent	68	55	61	58	
Present	56	45	44	42	
Venous invasion					0.38
Absent	114	92	92	88	
Present	10	8	12	12	
Stage					0.29
Stage 0-I	32	25	33	32	
Stage II-IV	92	75	73	68	

*1 SD; Standard deviation.

and 3 cases of stage IV. The stage classification was based on TNM classification on malignant tumor 7th edition by UICC.

Evaluation of miR-15a expression in clinical samples. The resected tumor tissue specimens were immediately frozen in liquid nitrogen and kept at –80°C until analysis. Total RNA extraction from primary tumors was performed as previously described (9). We synthesized *miR-15a*-specific cDNAs from total RNA using gene-specific primers according to the TaqMan MicroRNA Assays Protocol (Roche Applied Science, Indianapolis, USA). Reverse transcription as well as Real-Time PCR detection were carried-out using hsa-miR-15a-5p (Assay ID: 000389; Applied Biosystems, USA). RNU6B (Assay ID: 001093; Applied Biosystems, USA) was used as a reference gene. Quantitative real-time reverse transcriptase-polymerase chain reaction (RT-PCR) was performed using Applied Biosystems 7500 real-time PCR system, as previously described (9). The raw data of miRNA expression was normalized by RNU6B and calculated as relative quantification of miRNA expression values to that of one case in our samples. Before sample acquisition, each patient provided written informed consent. This study was approved by the ethics committees of Kyushu University.

Table II. *Results of the multivariate analysis between clinicopathological factors and overall survival (Cox proportional hazard model).*

Factors	RR (95% CI)	*p*-Value
Age	3.79 (0.55-27.4)	0.18
ER (positive/negative)	0.50 (0.14-1.93)	0.31
PgR (positive/negative)	7.34 (1.87-29.6)	0.004*
HER2 (positive/negative)	1.15 (0.49-2.84)	0.75
T factor (Tis-1/T2-T4)	3.14 (0.39-19.5)	0.47
Lymph node metastasis (negative/positive)	1.15 (0.13-24.9)	0.09
Lymphatic invasion (negative/positive)	11.4 (0.61-743)	0.86
Venous invasion (negative/positive)	2.59 (0.56-12.7)	0.67
Nuclear Grade (1-2/3)	1.72 (0.75-3.91)	0.20
Stage(0-1/2-4)	3.40 (0.36-76.2)	0.30
miR-15a expression (high/low)	2.56 (1.03-7.18)	0.04*

Statistical analysis. For the analysis of *miR-15a*, differences between clinicopathological factors were analyzed by χ^2 tests for categorial variables. Disease-free survival and overall survival time were measured from the first operation until the date of death or last follow-up. Survival curves were determined using the Kaplan-Meier method and statistical significance between groups was assessed using the wilcoxon test. Multivariate analysis was performed to assess the relative influence of prognostic factors on overall survival, using the Cox proportional hazards model in a forward stepwise procedure. Statistical analysis was performed by JMP® Pro 9.0.2 for Mac OS (SAS Institute).

Results

Low miR-15a expression in the primary tumor is a prognostic factor for BC patients. *MiR-15a* expression in the primary tumor was assessed in 230 patients with BC and divided into two groups according to their level of *miR-15a* expression. Analysis of clinicopathological factors in relation to *miR-15a* expression levels revealed no significant correlation (Table I). Patients in the low-*miR-15a* expression group had a significantly shorter term of disease-free survival than those in the high-*miR-15a* expression group (Figure 1a). However, there was no significant correlation between high and low expression levels of *miR-15a* and overall survival. In ER-positive and HER2-positive cases, there was no correlation between *miR-15a* expression and disease-free survival or overall survival (Figure 3). In triple-negative cases, low *miR-15a* expression was significantly correlated with shorter disease-free survival (p=0.0012) and overall survival (p=0.005) (Figure 2).

Multivariate analysis of overall survival showed that the level of *miR-15a* expression was an independent prognostic predictor [relative risk (RR)=2.56; 95% confidence interval (CI), 1.03-7.18; p=0.004] by Cox proportional hazards model] (Table II). PgR was also shown to be an independent prognostic predictor (RR=7.34; 95%CI=1.87-29.6; p=0.004).

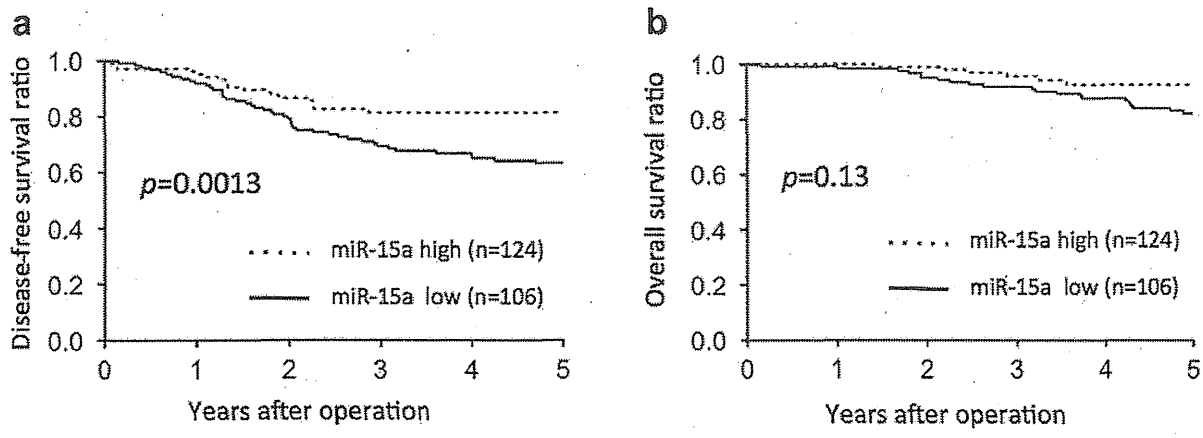

Figure 1. *Kaplan-Meier disease-free survival curve (a) and overall survival curve (b) of breast cancer cases based on the level of miR-15a in primary tumor.*

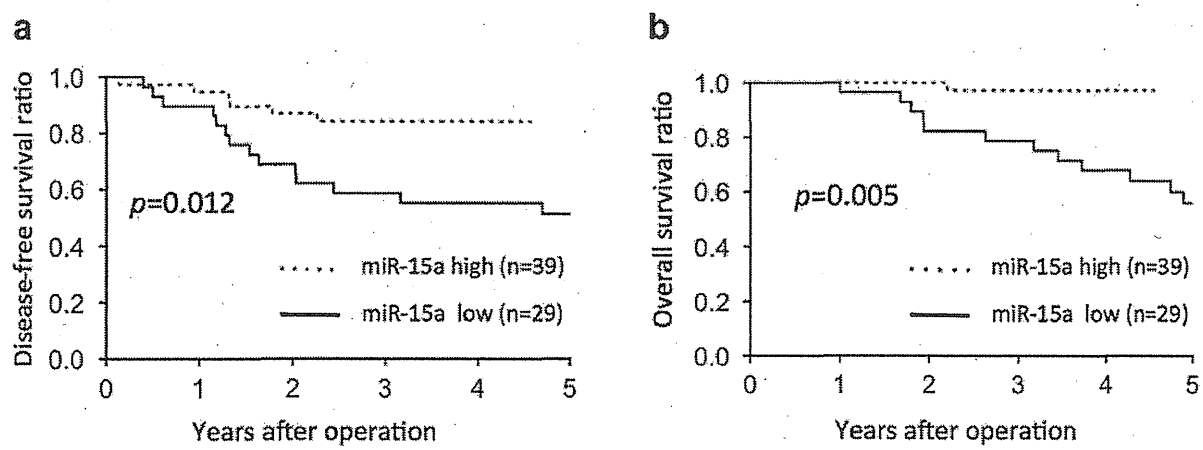

Figure 2. *Kaplan-Meier disease-free survival curve (a) and overall survival curve (b) of triple-negative breast cancer cases based on the level of miR-15a in primary tumor.*

Discussion

In the present study, we demonstrated that low *miR-15a* expression correlated with poor prognosis for patients with BC, particularly in triple-negative cases. It is known that *miR-15a* has many targets and is involved in several cancer pathways. Luo *et al.* reported that *miR-15a* targets *CCNE1*, which regulates the G_0 to G_1 phase transition and promotes cell-cycle progression. They reported that the up-regulation of *miR-15a* led to an increased number of cells in the G_0/G_1 phase, reduced cells in the S and G_2/M phases, and inhibited cell proliferation and migration (7). They also demonstrated the tumor suppressive activity of *miR-15a* in a breast cancer cell line. In addition, Liu *et al.* reported that the up-regulation of several miRNAs, including *miR-15a*, led to the down-regulation of *Smurf2*, which is known to play a complex role in tumorigenesis (8). However, Kodahl *et al.* reported that measurement of the expression of a combination of several miRNAs, including *miR-15a*, was able to discriminate between ER-positive BC patients and healthy controls (10). Interestingly, they found *miR-15a* expression was high in BC patients compared to healthy controls, suggesting perhaps an oncogenic role for *miR-15a*. The results of the present study support the hypothesis that *miR-15a* has a tumor-suppressive effect in breast cancer cases. With regard to specific subtypes of breast cancer, we

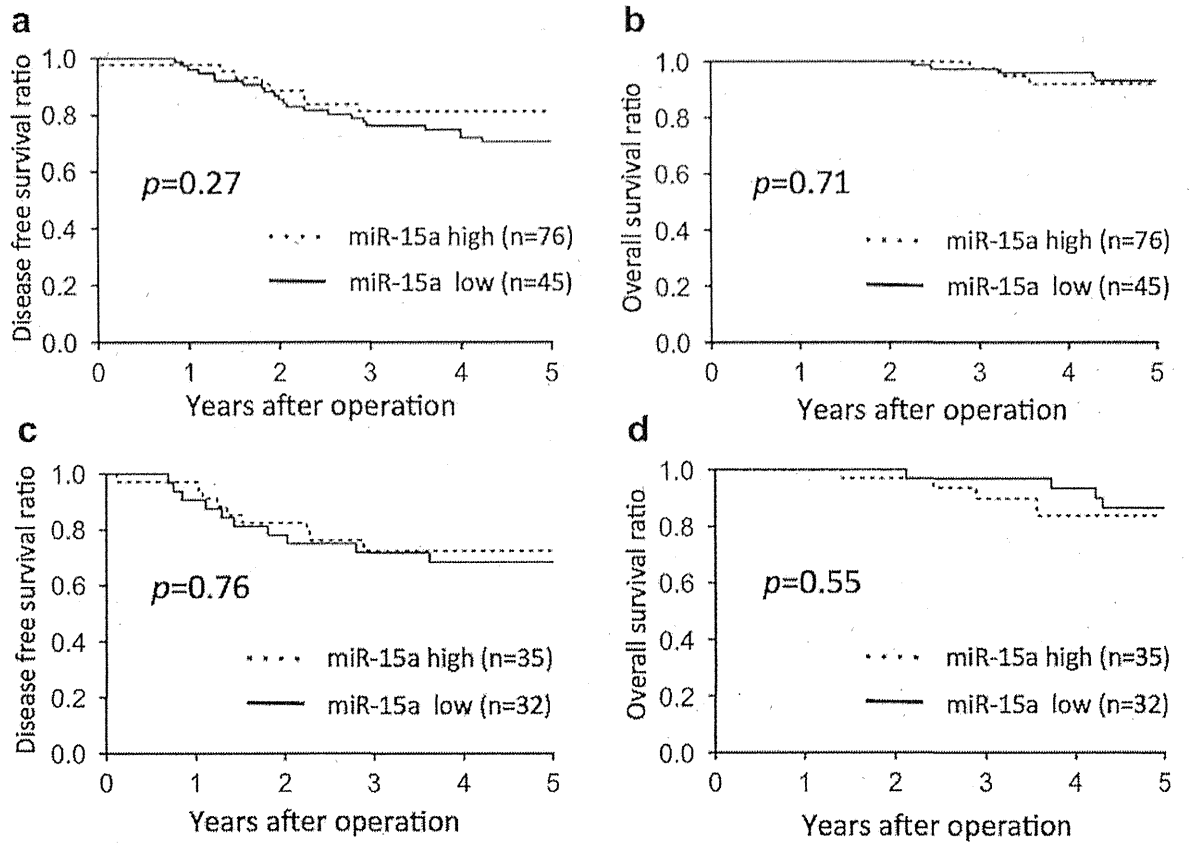

Figure 3. *Kaplan-Meier disease-free survival curve (a) and overall survival curve (b) in ER-positive breast cancer cases based on the level of miR-15a in primary tumor. Disease-free survival curve (c) and overall survival curve (d) in ER-negative breast cancer cases based on the level of miR-15a in primary tumor.*

found a significant correlation between *miR-15a* expression and poor prognosis in triple-negative cases. The relationship between *miR-15a* and *Smurf2* in triple-negative BC (8) has also been demonstrated by Liu *et al.*, and it was also suggested that genes like *Smurf2* targeted by *miR-15a* have critical roles in triple-negative BC.

In the present study, we found that in addition to *miR-15a* expression, the PgR expression was an independent prognostic predictor (RR=7.34; 95%CI=1.87-29.6; p=0.004). Although it is well-known that PgR-negative cases have a poorer prognosis than PgR-positive cases in luminar BC (11, 12), the significance of PgR expression status seemed to be overestimated in our study. Although it is possible that the nature of our samples produced some bias, the significant correlation between *miR-15a* and poor prognosis seems to be independent of PgR due to finding no significant correlation between the expression levels of *miR-15a* and PgR expression status (Table I).

In conclusion, *miR-15a* expression in BC primary tumors was an independent prognostic factor for overall survival; low *miR-15a* in the primary tumor predicted a poor prognosis for BC patients. In triple-negative patients, a low level of *miR-15a* expression was significantly correlated with shorter disease-free survival and overall survival.

Acknowledgements

The Authors would like to thank K. Oda, M. Kasagi, and S. Kono for their technical assistance. This work was supported in part by the Japan Society for the Promotion of Science (25830102).

References

1 Serpico D, Molino L and Di Cosimo S: microRNAs in breast cancer development and treatment. Cancer Treat Rev *40*: 595-604, 2014.
2 Calin GA and Croce CM: MicroRNA signatures in human cancers. Nat Rev Cancer *6*: 857-866, 2006.

3 Iorio MV, Ferracin M, Liu CG, Veronese A, Spizzo R, Sabbioni S, Magri E, Pedriali M, Fabbri M, Campiglio M, Menard S, Palazzo JP, Rosenberg A, Musiani P, Volinia S, Nenci I, Calin GA, Querzoli P, Negrini M and Croce CM: MicroRNA gene expression deregulation in human breast cancer. Cancer Res *65*: 7065-7070, 2005.

4 Dong C, Ji M and Ji C: microRNAs and their potential target genes in leukemia pathogenesis. Cancer Biol Ther *8*: 200-205, 2009.

5 Tivnan A and McDonald KL: Current progress for the use of miRNAs in glioblastoma treatment. Mol Neurobiol *48*: 757-768, 2013.

6 Tang J, Ahmad A and Sarkar FH: The Role of MicroRNAs in Breast Cancer Migration, Invasion and Metastasis. International journal of molecular sciences *13*: 13414-13437, 2012.

7 Luo Q, Li X, Li J, Kong X, Zhang J, Chen L, Huang Y and Fang L: MiR-15a is underexpressed and inhibits the cell cycle by targeting CCNE1 in breast cancer. Int J Oncol *43*: 1212-1218, 2013.

8 Liu X, Gu X, Sun L, Flowers AB, Rademaker AW, Zhou Y and Kiyokawa H: Downregulation of Smurf2, a tumor-suppressive ubiquitin ligase, in triple-negative breast cancers: involvement of the RB-microRNA axis. BMC cancer *14*: 57, 2014.

9 Ota D, Mimori K, Yokobori T, Iwatsuki M, Kataoka A, Masuda N, Ishii H, Ohno S and Mori M: Identification of recurrence-related microRNAs in the bone marrow of breast cancer patients. Int J Oncol *38*: 955-962, 2011.

10 Kodahl AR, Lyng MB, Binder H, Cold S, Gravgaard K, Knoop AS and Ditzel HJ: Novel circulating microRNA signature as a potential non-invasive multi-marker test in ER-positive early-stage breast cancer: A case control study. Mol Oncol *8*: 874-883, 2014.

11 Goldhirsch A, Winer EP, Coates AS, Gelber RD, Piccart-Gebhart M, Thurlimann B, Senn HJ and Panel M: Personalizing the treatment of women with early breast cancer: highlights of the St Gallen International Expert Consensus on the Primary Therapy of Early Breast Cancer 2013. Annals of oncology: official journal of the European Society for Medical Oncology/ ESMO *24*: 2206-2223, 2013.

12 Prat A, Cheang MC, Martin M, Parker JS, Carrasco E, Caballero R, Tyldesley S, Gelmon K, Bernard PS, Nielsen TO and Perou CM: Prognostic significance of progesterone receptor-positive tumor cells within immunohistochemically defined luminal A breast cancer. J Clin Oncol *31*: 203-209, 2013.

Received August 26, 2014
Revised October 5, 2014
Accepted October 10, 2014

Instructions to Authors 2015

General Policy. ANTICANCER RESEARCH (AR) will accept original high quality works and reviews on all aspects of experimental and clinical cancer research. The Editorial Policy suggests that priority will be given to papers advancing the understanding of cancer causation, and to papers applying the results of basic research to cancer diagnosis, prognosis, and therapy. AR will also accept the following for publication: (a) Abstracts and Proceedings of scientific meetings on cancer, following consideration and approval by the Editorial Board; (b) Announcements of meetings related to cancer research; (c) Short reviews (of approximately 120 words) and announcements of newly received books and journals related to cancer, and (d) Announcements of awards and prizes.

The principal aim of AR is to provide prompt publication (print and online) for original works of high quality, generally within 1-2 months from final acceptance. Manuscripts will be accepted on the understanding that they report original unpublished works on the cancer problem that are not under consideration for publication by another journal, and that they will not be published again in the same form. All authors should sign a submission letter confirming the approval of their article contents. All material submitted to AR will be subject to review, when appropriate, by two members of the Editorial Board and by one suitable outside referee. The Editors reserve the right to improve manuscripts on grammar and style.

The Editors and Publishers of AR accept no responsibility for the contents and opinions expressed by the contributors. Authors should warrantee due diligence in the creation and issuance of their work.

NIH Open Access Policy. The journal acknowledges that authors of NIH funded research retain the right to provide a copy of the final manuscript to the NIH four months after publication in ANTICANCER RESEARCH, for public archiving in PubMed Central.

Copyright. Once a manuscript has been published in ANTICANCER RESEARCH, which is a copyrighted publication, the legal ownership of all published parts of the paper has been transferred from the Author(s) to the journal. Material published in the journal may not be reproduced or published elsewhere without the written consent of the Managing Editor or Publisher.

Format. Two types of papers may be submitted: (i) Full papers containing completed original work, and (ii) review articles concerning fields of recognisable progress. Papers should contain all essential data in order to make the presentation clear. Reasonable economy should be exercised with respect to the number of tables and illustrations used. Papers should be written in clear, concise English. Spelling should follow that given in the "Shorter Oxford English Dictionary".

Manuscripts. Submitted manuscripts should not exceed fourteen (14) pages (approximately 250 words per double - spaced typed page), including abstract, text, tables, figures, and references (corresponding to 4 printed pages). Papers exceeding four printed pages will be subject to excess page charges. All manuscripts should be divided into the following sections:
(a) *First page* including the title of the presented work [not exceeding fifteen (15) words], full names and full postal addresses of all Authors, name of the Author to whom proofs are to be sent, key words, an abbreviated running title, an indication "review", "clinical", "epidemiological", or "experimental" study, and the date of submission. (Note: The order of the Authors is not necessarily indicative of their contribution to the work. Authors may note their individual contribution(s) in the appropriate section(s) of the presented work); (b) *Abstract* not exceeding 150 words, organized according to the following headings: Background/Aim - Materials and Methods/Patients and Methods - Results - Conclusion; (c) *Introduction;* (d) *Materials and Methods/Patients and Methods;* (e) *Results;* (f) *Discussion;* (g) *Acknowledgements;* (h) *References*. All pages must be numbered consecutively. Footnotes should be avoided. Review articles may follow a different style according to the subject matter and the Author's opinion. Review articles should not exceed 35 pages (approximately 250 words per double-spaced typed page) including all tables, figures, and references.

Figures. All figures (whether photographs or graphs) should be clear, high contrast, at the size they are to appear in the journal: 8.00 cm (3.15 in.) wide for a single column; 17.00 cm (6.70 in.) for a double column; maximum height: 20.00 cm (7.87 in.). Graphs must be submitted as photographs made from drawings and must not require any artwork, typesetting, or size modifications. Symbols, numbering and lettering should be clearly legible. The number and top of each figure must be indicated. Colour plates are charged.

Tables. Tables should be typed double-spaced on a separate page, numbered with Roman numerals and should include a short title.

References. Authors must assume responsibility for the accuracy of the references used. Citations for the reference sections of submitted works should follow the standard form of "Index Medicus" and must be numbered consecutively. In the text, references should be cited by number. Examples: 1 Sumner AT: The nature of chromosome bands and their significance for cancer research. Anticancer Res 1: 205-216, 1981. 2 McGuire WL and Chamnes GC: Studies on the oestrogen receptor in breast cancer. In: Receptors for Reproductive Hormones (O' Malley BW, Chamnes GC (eds.). New York, Plenum Publ Corp., pp 113-136, 1973.

Nomenclature and Abbreviations. Nomenclature should follow that given in "Chemical Abstracts", "Index Medicus", "Merck Index", "IUPAC –IUB", "Bergey's Manual of Determinative Bacteriology", The CBE Manual for Authors, Editors and Publishers (6th edition, 1994), and MIAME Standard for Microarray Data. Human gene symbols may be obtained from the HUGO Gene Nomenclature Committee (HGNC) (http://www.gene.ucl.ac.uk/). Approved mouse nomenclature may be obtained from http://www.informatics.jax.org/. Standard abbreviations are preferable. If a new abbreviation is used, it must be defined on first usage.

Clinical Trials. Authors of manuscripts describing clinical trials should provide the appropriate clinical trial number in the correct format in the text.
For International Standard Randomised Controlled Trials (ISRCTN) Registry (a not-for-profit organization whose registry is administered by Current Controlled Trials Ltd.) the unique number must be provided in this format: ISRCTNXXXXXXXX (where XXXXXXXX represents the unique number, always prefixed by "ISRCTN"). Please note that there is no space between the prefix "ISRCTN" and the number. Example: ISRCTN47956475.

For Clinicaltrials.gov registered trials, the unique number must be provided in this format: NCTXXXXXXXX (where XXXXXXXX represents the unique number, always prefixed by 'NCT'). Please note that there is no space between the prefix 'NCT' and the number. Example: NCT00001789.

Ethical Policies and Standards. ANTICANCER RESEARCH agrees with and follows the "Uniform Requirements for Manuscripts Submitted to Biomedical Journals" established by the International Committee of Medical Journal Editors in 1978 and updated in October 2001 (www.icmje.org). Microarray data analysis should comply with the "Minimum Information About Microarray Experiments (MIAME) standard". Specific guidelines are provided at the "Microarray Gene Expression Data Society" (MGED) website. Presentation of genome sequences should follow the guidelines of the NHGRI Policy on Release of Human Genomic Sequence Data. Research involving human beings must adhere to the principles of the Declaration of Helsinki and Title 45, U.S. Code of Federal Regulations, Part 46, Protection of Human Subjects, effective December 13, 2001. Research involving animals must adhere to the Guiding Principles in the Care and Use of Animals approved by the Council of the American Physiological Society. The use of animals in biomedical research should be under the careful supervision of a person adequately trained in this field and the animals must be treated humanely at all times. Research involving the use of human foetuses, foetal tissue, embryos and embryonic cells should adhere to the U.S. Public Law 103-41, effective December 13, 2001.

Submission of Manuscripts. Please follow the Instructions to Authors regarding the format of your manuscript and references. There are 3 ways to submit your article (NOTE: Please use only one of the 3 options. Do not send your article twice.):

1. To submit your article online please visit: IIAR-Submissions (http://www.iiar-anticancer.org/submissions/login.php)
2. You can send your article via e-mail to journals@iiar-anticancer.org. Please remember to always indicate the name of the journal you wish to submit your paper. The text should be sent as a Word document (*doc) attachment. Tables, figures and cover letter can also be sent as e-mail attachments.
3. You can send the manuscript of your article via regular mail in a USB stick, DVD, CD or floppy disk (including text, tables and figures) together with three hard copies to the following address:
   John G. Delinasios
   International Institute of Anticancer Research (IIAR)
   Editorial Office of ANTICANCER RESEARCH,
   IN VIVO, CANCER GENOMICS and PROTEOMICS.
   1st km Kapandritiou-Kalamou Road
   P.O. Box 22, GR-19014 Kapandriti, Attiki
   GREECE

Submitted articles will not be returned to Authors upon rejection.

Galley Proofs. Unless otherwise indicated, galley proofs will be sent to the first-named Author of the submission. Corrections of galley proofs should be limited to typographical errors. Reprints, PDF files, and/or Open Access may be ordered after the acceptance of the paper. Requests should be addressed to the Editorial Office.

Ann Surg Oncol
DOI 10.1245/s10434-015-4418-2

Annals of
SURGICAL ONCOLOGY
OFFICIAL JOURNAL OF THE SOCIETY OF SURGICAL ONCOLOGY

ORIGINAL ARTICLE – TRANSLATIONAL RESEARCH AND BIOMARKERS

The *miR-506*-Induced Epithelial–Mesenchymal Transition is Involved in Poor Prognosis for Patients with Gastric Cancer

Shotaro Sakimura, MD[1,2], Keishi Sugimachi, MD, PhD[1], Junji Kurashige, MD, PhD[1], Masami Ueda, MD[1], Hidenari Hirata, MD[1], Sho Nambara, MD[1], Hisateru Komatsu, MD[1], Tomoko Saito, MD[1], Yuki Takano, MD[1], Ryutaro Uchi, MD[1], Etsuko Sakimura, MD[1], Yoshiaki Shinden, MD[1], Tomohiro Iguchi, MD, PhD[1], Hidetoshi Eguchi, MD, PhD[1], Yugo Oba, MD[2], Sumio Hoka, MD, PhD[2], and Koshi Mimori, MD, PhD[1]

[1]Department of Surgery, Kyushu University Beppu Hospital, Beppu, Japan; [2]Department of Anesthesiology and Critical Care Medicine, Graduate School of Medical Sciences, Kyushu University, Fukuoka, Japan

ABSTRACT

Background. MicroRNAs have roles in the regulation of the epithelial–mesenchymal transition (EMT). Findings have shown that *miR-506* inhibits the expression of *SNAI2*, and that low expression of *miR-506* is associated with poor prognoses in ovarian and breast cancers. This study investigated the role of *miR-506* in survival and the EMT in patients with gastric cancer.

Methods. In this study, *miR-506* and *SNAI2* mRNA levels were measured in 141 cases of gastric cancer by quantitative reverse transcription polymerase chain reaction, and the protein expressions of SNAI2 and E-cadherin in 39 cases were validated by immunohistochemical analysis. Next, the associations between their expression levels and clinicopathologic factors were evaluated. In addition, cell proliferation, migration, and luciferase activity of the 3′ untranslated region (UTR) of *SNAI2* were analyzed using pre-*miR-506* precursor in two human gastric cancer cell lines.

Results. Low expression of *miR-506* was significantly correlated with poor overall survival in both the univariate analysis ($P = 0.016$) and the multivariate analysis ($P < 0.05$). Low *miR-506* expression was significantly correlated with high *SNAI2* expression ($P = 0.009$) and poorly differentiated type ($P = 0.015$). In vitro, *miR-506* suppressed *SNAI2* expression by binding to its 3′UTR, resulting in increased expression of *E-cadherin* ($P < 0.05$), verified by immunohistochemical analysis. Pre-*miR-506* transfected cells showed significantly suppressed cell proliferation and migration ($P < 0.05$) compared with the control cells.

Conclusions. The EMT was directly suppressed by *miR-506*, and its low expression was an independent prognostic factor in gastric cancer patients. The data indicated that *miR-506* may act as a tumor suppressor and could be a novel therapeutic agent.

Gastric cancer is the fifth most common malignant tumor in the world and the third leading cause of cancer death worldwide. The incidence of gastric cancer and the resulting mortality have decreased worldwide, especially in developed countries, primarily because of better living conditions and improvements in diagnosis and treatment. However, gastric cancer remains a challenge in East Asia, with high incidence and mortality rates persisting.[1,2] Gastric cancer is difficult to cure unless it is found at an early stage because few symptoms are manifested during the early stage, and the disease usually is advanced when the diagnosis is determined.

The epithelial–mesenchymal transition (EMT) is a process through which epithelial cells lose their cell polarity and cell–cell adhesion and gain migratory and invasive properties to become mesenchymal cells.[3] The EMT, reported to play important roles in the progression and metastasis of cancer, is associated with a poor prognosis.[4] E-cadherin is required for the maintenance of cell adhesion, and lack of E-cadherin expression is important for the

Electronic supplementary material The online version of this article (doi:10.1245/s10434-015-4418-2) contains supplementary material, which is available to authorized users.

First Received: 1 July 2014

K. Mimori, MD, PhD
e-mail: kmimori@beppu.kyushu-u.ac.jp

Published online: 24 February 2015

EMT. Downregulation of E-cadherin expression due to mutation, deletion, CpG hypermethylation, or SNAI-mediated transcriptional repression of the *CDH-1* gene, which encodes E-cadherin, leads to the EMT in gastric cancer.[5–7]

MicroRNAs (miRNAs) are small noncoding RNAs of 20–25 nucleotides that bind to the 3′ untranslated region (UTR) of multiple-target mRNAs, enhancing their degradation and inhibiting their translation. Reports show an association of MiRNAs with a variety of diseases, including cancer.[8,9] Recent studies have shown that miRNAs regulate not only proliferation, differentiation, and migration,[10] but also the EMT by suppressing EMT-related transcription factors in cancer cells.[11,12]

Peritoneal metastasis, the most frequent pattern of metastasis, has been shown to correlate with poor prognosis in advanced gastric cancer.[13,14] Some studies have shown that the EMT plays a crucial role in the formation of peritoneal metastases by gastric cancer cells.[15,16] Therefore, it is necessary to elucidate the epigenetic mechanisms of the EMT to improve early diagnosis and treatment of peritoneal metastases.

Recent studies have shown that *miR-506* controls the EMT by inhibiting the expression of SNAI2 and PRRX1 and that aberrant low expression of *miR-506* is associated with a poor prognosis in ovarian and breast cancers.[17,18] However, the importance of *miR-506* expression as a prognostic factor for the EMT and peritoneal metastasis has not been studied in gastric cancer to date. Therefore, the current study investigated the role of *miR-506* in the survival of Japanese patients with gastric cancer and analyzed the function of *miR-506* in the EMT in gastric cancer cell lines.

MATERIALS AND METHODS

Patients

This study enrolled 141 patients with gastric cancer who underwent gastrectomy at Kyushu University Beppu Hospital and affiliated hospitals between 1989 and 2009. Written informed consent was obtained from all the patients in accordance with the guidelines approved by the Institutional Research Board. This study was conducted under the supervision of the ethical board of Kyushu University and affiliated hospitals. Detailed information is described in the Supplementary Material.

Cell Lines

The human gastric cancer cell lines MKN7 and MKN45 were obtained from the Riken Bioresource Center (Tsukuba, Japan) and maintained in RPMI 1640 medium containing 10 % fetal bovine serum, 100 U/mL penicillin, and 100 μg/mL streptomycin sulfate. Cells were cultured at 37 °C in a humidified atmosphere containing 5 % carbon dioxide (CO_2).

Transfection with miR-506 Precursor (pre-miR-506)

Cells were transfected with either pre-*miR-506* or pre-*miR*-negative control (Ambion, Austin, TX, USA) using Lipofectamine RNAiMAX (Invitrogen Life Technologies, Carlsbad, CA, USA) according to the manufacturer's instructions.

Preparation of RNA for Reverse-Transcription Polymerase Chain Reaction

Total RNA was isolated using a modified acid-guanidine-phenol–chloroform procedure, as described previously.[19] Complementary DNA (cDNA) was synthesized from 8 μg total RNA using random hexamer primers and Moloney murine leukemia virus (M-MLV) reverse transcriptase (Invitrogen Life Technologies).

Evaluation of Gene and miRNA Expression in Clinical Samples

Quantitative reverse transcription polymerase chain reaction (qRT-PCR) was performed in a LightCycler 480 instrument (Roche Applied Science, Basel, Switzerland) using a LightCycler 480 Probes Master kit (Roche Applied Science). The detailed protocol and the primer sequences used in this procedure are described in the Supplementary Material.

Construction of Reporter Plasmids and Evaluation of Luciferase Reporter Activity

To construct a luciferase reporter plasmid, most of the length of the *SNAI2* 3′UTR, which contained the *miR-506* binding sites, was subcloned into the pmirGlo Dual-luciferase miRNA Target Expression Vector (Promega, Madison, WI, USA) located 5′ to the firefly luciferase. Nucleotide sequences of the constructed plasmids were confirmed by DNA-sequencing analysis. Detailed information is provided in the Supplementary Material.

Immunoblotting Analysis

Total cellular protein was extracted from MKN7 and MKN45 cells 48 h after transfection with pre-*miR-506*. Total protein (40 μg) was extracted from MKN cells and electroblotted as previously described.[20] Detailed information is provided in the Supplementary Material.

Immunohistochemical Analysis

Levels of E-cadherin and SNAI2 protein expression were measured by immunohistochemical analysis in 39 pathologic tissue samples available from 141 cases analyzed by RT-PCR. Formalin-fixed, paraffin-embedded tissue sections corresponding to the samples used for mRNA expression analysis were analyzed. Detailed information is provided in the Supplementary Material.

Cell Proliferation and Cell Migration Analysis

Cell proliferation was evaluated by MTT assay using a Cell Proliferation Kit 1 (Roche Applied Science) according to the manufacturer's instructions. Migration assays were conducted using the BD Falcon HTS Fluoro Block Insert (BD Biosciences, San Jose, CA, USA). Detailed information is provided in the Supplementary Material.

Statistical Analysis

Continuous variables are expressed as means ± standard deviations. Data were analyzed using JMP 9 software (JMP, Cary, NC, USA). Overall survival rates were calculated according to the Kaplan–Meier method, and the log-rank test was applied to compare the survival curves. Multivariate analysis for the survival was performed on the basis of the Cox proportional hazards model. The relationship between groups was analyzed using the Chi square test and Fisher's test. Continuous variables between two groups were analyzed using Student's t test after experiments had been repeated at least three times. A probability level of 0.05 was chosen for statistical significance.

RESULTS

Clinicopathologic Significance of miR-506 Expression in Gastric Cancer

Expression of *miR-506* was examined in 141 tumors by qRT-PCR to investigate the clinical significance of *miR-506* in gastric cancer. Cases were subdivided into two groups [a low-expression group ($n = 85$) and a high-expression group ($n = 56$)] according to the level of *miR-506* expression. These groups were classified using the minimum P value approach, which is a comprehensive method for finding the optimal risk separation cutoff point in continuous measurements.[21] Clinicopathologic factors then were analyzed between the two groups (Supplementary Table 1). The group with low *miR-506* expression contained significantly more poorly differentiated grades than the group with high *miR-506* expression ($P = 0.015$). The patients with low *miR-506* expression divided by the median value of *miR-506* also tended to have a lower survival rate than those with high expression ($P = 0.051$, data not shown).

With regard to overall survival, the patients with low *miR-506* expression had a significantly lower survival rate than those with high expression ($P = 0.0160$; Fig. 1a). We also performed subgroup analysis of the patients without peritoneum metastasis ($n = 118$). The patients with low *miR-506* expression also had a significantly lower survival rate in this subgroup ($P = 0.0096$; Fig. 1b). Uni- and multivariate analyses for overall survival showed that *miR-*

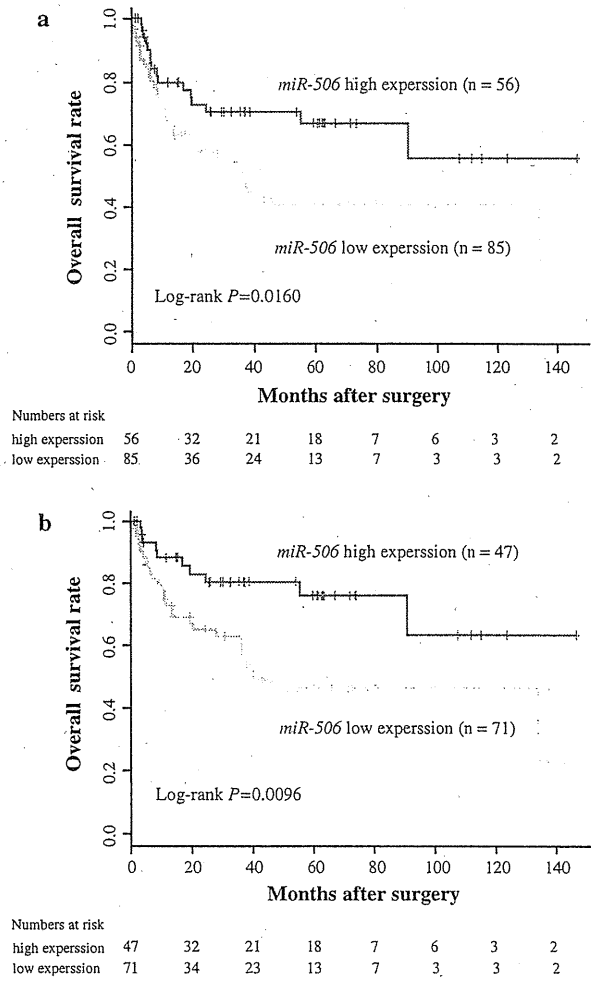

FIG. 1 The low expression of *miR-506* was significantly correlated with poor overall survival. Kaplan–Meier overall survival curves according to *miR-506* expression levels are shown. **a** The overall survival of patients with low *miR-506* expression ($n = 85$) was significantly lower than that of patients with high expression ($n = 56$; $P = 0.0160$, log-rank test). **b** The overall survival of patients with low *miR-506* expression ($n = 71$) was significantly lower than that of patients with high expression ($n = 47$) among the patients without peritoneum metastasis ($P = 0.0096$, log-rank test)

TABLE 1 Uni- and multivariate analyses of clinicopathologic features for overall survival (Cox proportional regression model)

Features	Univariate analysis			Multivariate analysis		
	HR	95 % CI	*P* Value	HR	95 % CI	*P* Value
Age (>70/≤70)	0.626	0.345–1.089	0.099	1.830	1.031–3.384	0.039
Gender (male/female)	1.491	0.844–2.781	0.174	1.964	1.084–3.743	0.025
Histologic grade (well & moderately/poorly & nondifferentiated)[a]	1.647	0.959–2.892	0.071	1.295	0.718–2.375	0.392
Depth of the tumor (T1, 2/T3, 4)	4.957	2.389–12.040	<0.001	2.013	0.742–6.277	0.177
Lymph node metastasis (absent/present)	5.363	2.581–13.038	<0.001	3.078	1.270–8.564	0.011
Venous invasion (absent/present)	3.164	1.859–5.420	<0.001	1.159	0.606–2.215	0.654
Peritoneum metastasis (absent/present)	4.933	2.635–8.928	<0.001	3.281	1.632–6.530	0.001
Stages 1, 2/3, 4	5.429	2.948–10.780	<0.001	–	–	–
miR-506 expression (low/high)	2.017	1.149–3.713	0.014	1.899	1.053–3.588	0.033

Staging was classified by the Union for International Cancer Control (UICC), 7th edition

HR hazard ratio, *CI* confidence interval

[a] Well (well-differentiated adenocarcinoma, moderately (moderately differentiated adenocarcinoma), poorly (poorly differentiated adenocarcinoma, nondifferentiated (nondifferentiated adenocarcinoma)

506 expression was an independent and significant prognostic factor (relative risk 1.78; 95 % confidence interval, 1.00–3.30; $P = 0.049$; Table 1).

Regulation of SNAI2 Expression by miR-506 in Gastric Cancer

We next explored the potential target genes of *miR-506* in gastric cancer. Using TargetScan, an online tool available at http://www.targetscan.org/vert_50/, we identified a potential *miR-506* binding site in the 3′UTR of the transcript encoding SNAI2 (Supplementary Fig. 1). A luciferase reporter assay was conducted for direct investigation of binding and repression between *miR-506* and *SNAI2*. Transient cotransfection of MKN7 and MKN45 cells with the reporter plasmid and pre-*miR-506* significantly reduced luciferase activity compared with the negative control cells ($P < 0.05$; Fig. 2a). These data indicated that *SNAI2* mRNA is a direct functional target of *miR-506* in gastric cancer.

Endogenous miR-506 expression then was measured in three gastric cancer cell lines. Cell lines with high endogenous miR-506 expression (MKN-1 and NUGC-3) showed significantly lower SNAI2 expression than cells with low endogenous miR-506 expression (MKN-7) (Supplementary Fig. 2). Next, we sought to confirm that *miR-506* mediated the expression of *SNAI2* in two gastric cancer cell lines (MKN7 and MKN45) using pre-*miR-506*. We confirmed that *miR-506* expression in cells transfected with pre-*miR-506* was significantly higher than in cells transfected with pre-*miR*-negative control using qRT-PCR ($P < 0.05$; Supplementary Fig. 3). Moreover, *SNAI2* expression was significantly suppressed in MKN7 cells exposed to pre-*miR-506* ($P < 0.05$; Fig. 2b). In MKN45 cells transfected with pre-*miR-506*, the expression level of *SNAI2* tended to be suppressed, but this difference was not statistically significant due to the low basal expression of this target (Fig. 2b).

To investigate the function of *miR-506* in the EMT, we examined the expression level of the epithelial marker, *E-cadherin,* after overexpression of *miR-506* in gastric cancer cells. As shown in Fig. 2c, MKN7 cells transfected with pre-*miR-506* exhibited significantly increased expression of E-cadherin mRNA and protein.

Moreover, in clinical samples, the group with high *miR-506* mRNA expression exhibited significantly lower *SNAI2* expression than the group with low *miR-506* expression ($P = 0.009$; Fig. 2d). We explored the protein expression of SNAI2 in 39 gastric cancer patients. Immunohistochemical analysis showed that SNAI2 protein expression inversely correlated with *miR-506* mRNA expression, and the correlation was statistically significant ($P = 0.006$, Supplementary Table 2). Expression of SNAI2 was inversely correlated with E-cadherin expression in identical lesions of resected gastric cancer samples, as shown in Fig. 3. These data directly demonstrated that *miR-506* controlled the expression of *SNAI2* through binding to its 3′UTR and induced the EMT in gastric cancer.

Suppression of Cell Proliferation and Migration in Gastric Cancer by miR-506

Next, we evaluated the role of *miR-506* in determining the malignant potential of gastric cancer. Proliferation assays were conducted with gastric cancer cells transfected with pre-*miR-506* and with negative control cells. The

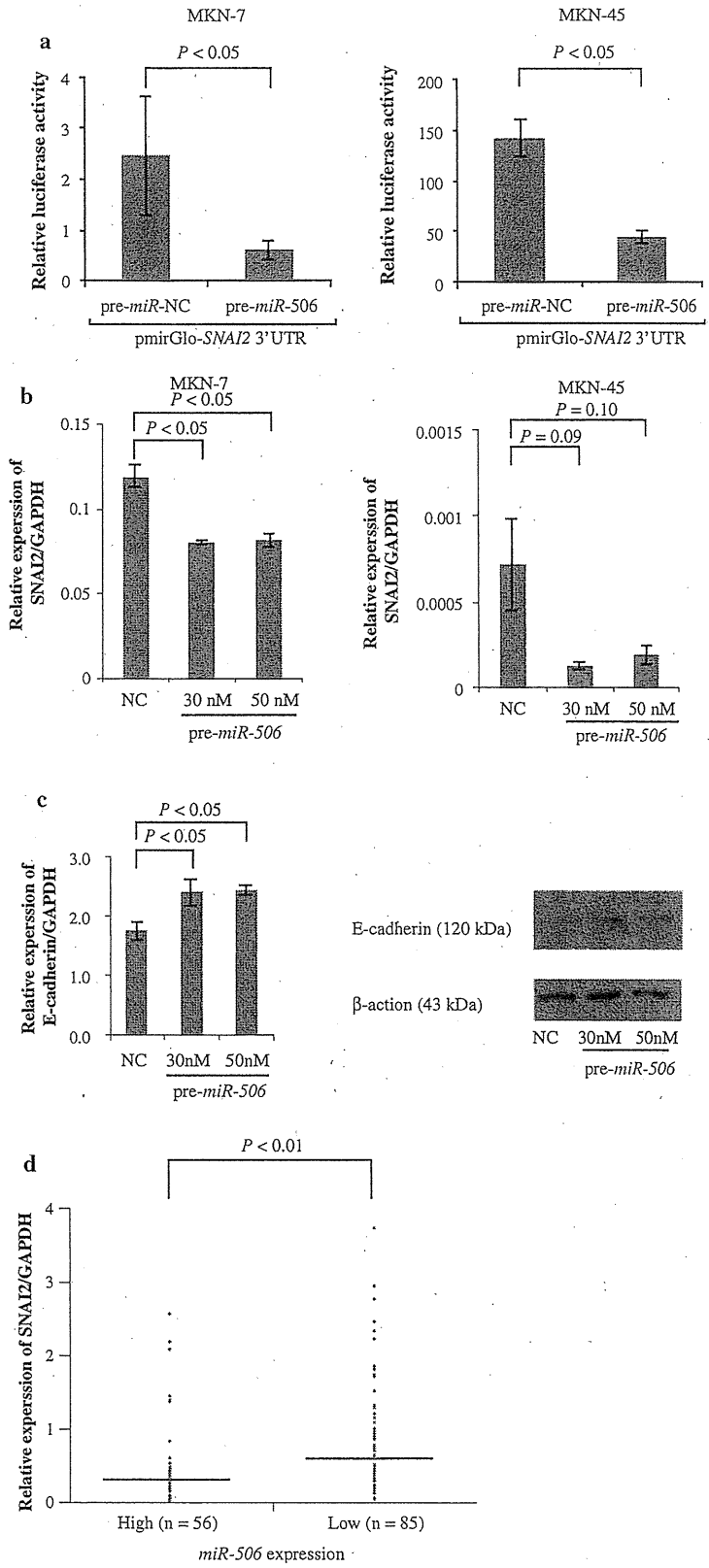

FIG. 2 In gastric cancer cell lines and samples from patients with gastric cancer, *miR-506* suppressed the expression of *SNAI2* and subsequently increased the expression of *E-cadherin*. **a** Luciferase assays demonstrated that *miR-506* repressed its target in MKN7 cells (*left*) and MKN45 cells (*right*) ($P < 0.05$). Relative luciferase level = [(sample Luc/sample Renilla)/(control Luc/control Renilla)]. *Luc*, raw firefly luciferase activity; *Renilla*, internal transfection control Renilla activity. The error bar represents the standard deviation (SD) from three replicates. **b** Expression of *SNAI2/GAPDH* as measured by quantitative real-time polymerase chain reaction (PCR) analysis in MKN7 cells (*left*) and MKN45 cells (*right*) after transfection with pre-*miR-506*. **c** Expression of E-cadherin transcripts and protein was measured by quantitative real-time PCR analysis and Western blot analysis, respectively, in MKN7 cells transfected with pre-*miR-506*. Protein expression was normalized to the expression of β-actin. **d** The group with high *miR-506* expression exhibited significantly lower *SNAI2* expression than the group with low expression ($P = 0.009$). Error bars represent the SD from three replicates. NC, pre-*miR* negative control; 30 nmol, pre-*miR-506* 30 nmol; 50 nmol, pre-*miR-506* 50 nmol

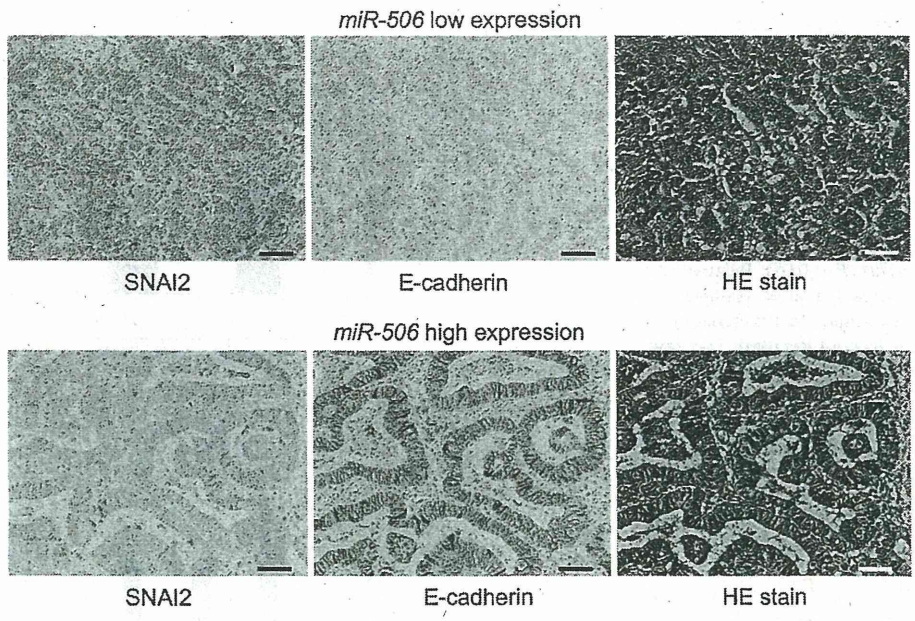

FIG. 3 Immunohistochemical analysis of clinical samples. Clinical samples showed an inverse correlation between the expression of SNAI2 and the expression of E-cadherin, as examined by immunohistochemical staining. *Scale bar*: 50 μm

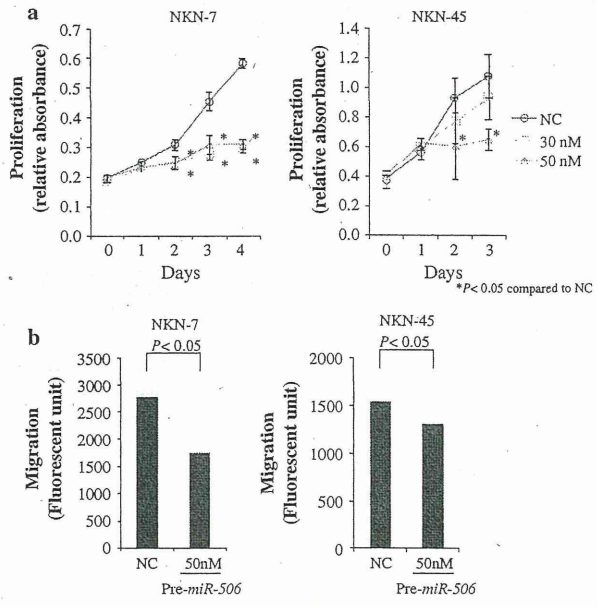

FIG. 4 Overexpression of *miR-506* suppressed the proliferation and migration of gastric cancer cells. As shown, *miR-506* significantly suppressed the **a** proliferation and **b** migratory capacity of gastric cancer cells compared with control cells ($P < 0.05$). Error bars represent the standard deviation from three replicates. NC, pre-*miR* negative control; 30 nmol, pre-*miR-506* 30 nmol; 50 nmol, pre-*miR-506* 50 nmol

findings showed that *miR-506* significantly suppressed the proliferation of both gastric cancer cell lines ($P < 0.05$; Fig. 4a). The expression of *miR-506* also significantly inhibited the migratory capacity of the cells compared with that of control cells ($P < 0.05$; Fig. 4b). These data demonstrated that impaired expression of *miR-506* promoted the malignant potential of gastric cancer.

DISCUSSION

In this study, the expression of *miR-506* was inversely correlated with the expression of *SNAI2* in clinical samples, and gastric cancer cell lines with *miR-506* overexpression exhibited decreased expression of *SNAI2* and increased expression of *E-cadherin*. Moreover, the study also provided direct evidence that *miR-506* suppresses *SNAI2* and that overexpression of *miR-506* significantly suppresses cell migration. This is the first report to show that *miR-506* controls the EMT by inhibiting *SNAI2* in gastric cancer.

Previous studies have shown that the EMT plays an important role in peritoneal metastasis.[15,16] In this study, however, we did not observe a relationship between the expression of *miR-506* and the incidence of peritoneal metastasis. The data indicated that although reduced expression of *miR-506* induces the EMT, other factors besides epigenetics are essential to the formation of peritoneal metastasis.[22,23]

Previous studies have shown that low expression of *miR-506* is associated with a poor prognosis in serous ovarian and breast cancers.[17,18] Consistent with this, our study initially showed that low expression of *miR-506* was an independent prognostic factor in gastric cancer patients. The low expression of *miR-506* was significantly correlated with poorer differentiation and more invasive properties. However, no significant relationships were found between the expression of *miR-506* and lymph node metastasis or

peritoneal metastasis. The group with low *miR-506* expression contained more undifferentiated histopathologic grades, which are characterized by more malignant, mesenchymal-like cells with low *E-cadherin* expression.[24,25] This indicates that *miR-506* is essential to maintain the differentiation of cancer cells and that loss of *miR-506* expression could lead to a poor prognosis.

In addition to its functions in the EMT, recent findings have shown that *miR-506* acts as a tumor suppressor. In lung cancer, ectopic expression of *miR-506* suppresses cell viability to induce the accumulation of reactive oxygen species (ROS),[26] and *miR-506* inhibits tumor growth by targeting the hedgehog pathway transcription factor *Gli3* and the *CDK4/6-FOXM1* axis in cervical cancer and ovarian cancer.[27,28] In our study, overexpression of *miR-506* by transfection with pre-*miR-506* significantly suppressed cell proliferation in gastric cancer cell lines, suggesting that *miR-506* may act as a tumor-suppressor miRNA to prevent gastric cancer progression.

Many miRNAs have been shown to control the EMT in various cancers.[29] For example, the *miR-200* family, *miR-30a*, and others have been shown to control the EMT by repressing the expression of EMT-related target proteins, such as *ZEB* or *Vimentin*.[12,30] It is possible that *miR-506* indirectly controls the EMT by pathways other than the *miR-506-SNAI2* axis. However, only one practical axis exists between *miR-506* and *SNAI2* because other EMT-related genes, such as *SNAI1*, *ZEB1*, and *ZEB2*, do not have binding sites for *miR-506* in their 3′UTRs.

Few studies have described the mechanisms through which *miR-506* expression is controlled in highly malignant cancers. One study showed that nuclear factor-κB (NF-κB) plays an important role in the EMT.[31] Additionally, NF-κB has been shown to suppress the expression of *miR-506* by binding to its promoter region in breast cancer.[18] Interestingly, genomic sequences upstream of *miR-506* may be putative p53-response elements. Consistent with this, p53 has been shown to promote the expression of *miR-506* in lung cancer.[26] In the current study, miR-506 was associated with proliferation and migration ability but was not correlated with invation and *p53* expression (data not shown). Therefore, further study is warranted to investigate another mechanism, such as amplification, deletion, or methylation, that controls the expression of *miR-506*.

In conclusion, this study showed that *miR-506* directly controlled the EMT by regulating *SNAI2* and was an independent prognostic factor in Japanese gastric cancer patients. Moreover, our data supported the conclusion that *miR-506* may act as a tumor suppressor in the context of gastric cancer. Because miRNAs have recently been recognized as potential therapeutic agents or targets in various diseases and because systemic delivery of synthetic miRNA has been shown to inhibit the growth of tumors,[32,33] we hypothesize that *miR-506* could be a potential therapeutic molecule in the treatment of gastric cancer. Further studies investigating the potential applications and significance of *miR-506* are ongoing.

ACKNOWLEDGMENT We thank K. Oda, M. Kasagi, S. Kohno, T. Kawano, and M. Aoyagi for their technical assistance. This work was supported in part by Japan Society for the Promotion of Science (JSPS) Grant-in-Aid for Scientific Research (Grant numbers 21591644, 21791295, 21791297, 215921014, and 21679006).

REFERENCES

1. IARC. GLOBOCAN 2012: Estimated cancer incidence, mortality and prevalence worldwide in 2012. Retrieved 10 January 2014 at http://globocan.iarc.fr/Pages/fact_sheets_cancer.aspx.
2. Hohenberger P, Gretschel S. Gastic cancer. *Lancet.* 2003; 362:305–15.
3. Thiery JP, Acloque H, Huang RY, Nieto MA. Epithelial–mesenchymal transitions in development and disease. *Cell.* 2009;139:871–90.
4. Thiery JP. Epithelial–mesenchymal transitions in tumour progression. *Nat Rev Cancer.* 2002;2:442–54.
5. Katoh M. Epithelial–mesenchymal transition in gastric cancer (review). *Int J Oncol.* 2005;27:1677–83.
6. Murai T, Yamada S, Fuchs BC, et al. Epithelial-to-mesenchymal transition predicts prognosis in clinical gastric cancer. *J Surg Oncol.* 2014;109:684–9.
7. Kaurah P, MacMillan A, Boyd N, et al. Founder and recurrent CDH1 mutations in families with hereditary diffuse gastric cancer. *J Am Med Assoc.* 2007;297:2360–72.
8. Bhayani MK, Calin GA, Lai SY. Functional relevance of miRNA sequences in human disease. *Mutat Res.* 2012;731:14–9.
9. Alvarez-Garcia I, Miska EA. MicroRNA functions in animal development and human disease. *Development.* 2005;132: 4653–62.
10. Calin GA, Croce CM. MicroRNA signatures in human cancers. *Nat Rev Cancer.* 2006;6:857–66.
11. Bouyssou JM, Manier S, Huynh D, Issa S, Roccaro AM, Ghobrial IM. Regulation of microRNAs in cancer metastasis. *Biochim Biophys Acta.* 2014;1845:255–65.
12. Song F, Yang D, Liu B, et al. Integrated microRNA network analyses identify a poor prognosis subtype of gastric cancer characterized by the miR-200 family. *Clin Cancer Res.* 2014;20:878–89.
13. Duarte I, Llanos O. Patterns of metastases in intestinal and diffuse types of carcinoma of the stomach. *Hum Pathol.* 1981; 12:237–42.
14. Maehara Y, Moriguchi S, Kakeji Y, et al. Pertinent risk factors and gastric carcinoma with synchronous peritoneal dissemination or liver metastasis. *Surgery.* 1991;110:820–3.
15. Okugawa Y, Inoue Y, Tanaka K, et al. Smad interacting protein 1 (SIP1) is associated with peritoneal carcinomatosis in intestinal type gastric cancer. *Clin Exp Metastasis.* 2013;30:417–29.
16. Okugawa Y, Toiyama Y, Tanaka K, et al. Clinical significance of zinc finger E-box binding homeobox 1 (ZEB1) in human gastric cancer. *J Surg Oncol.* 2012; 106:280–5.
17. Yang D, Sun Y, Hu L, et al. Integrated analyses identify a master microRNA regulatory network for the mesenchymal subtype in serous ovarian cancer. *Cancer Cell.* 2013;23:186–99.
18. Arora H, Qureshi R, Park WY. miR-506 regulates epithelial mesenchymal transition in breast cancer cell lines. *PloS One.* 2013;8:e64273.

19. Mori M, Mimori K, Yoshikawa Y, et al. Analysis of the gene-expression profile regarding the progression of human gastric carcinoma. *Surgery.* 2002;131:S39–47.
20. Ieta K, Ojima E, Tanaka F, et al. Identification of overexpressed genes in hepatocellular carcinoma, with special reference to ubiquitin-conjugating enzyme E2C gene expression. *Int J Cancer.* 2007;121:33–8.
21. Mizuno H, Kitada K, Nakai K, Sarai A. PrognoScan: a new database for meta-analysis of the prognostic value of genes. *BMC Med Genomics.* 2009;2:18.
22. Akagawa S, Ohuchida K, Torata N, et al. Peritoneal myofibroblasts at metastatic foci promote dissemination of pancreatic cancer. *Int J Oncol.* 2014;45:113–20.
23. Miyake S, Kitajima Y, Nakamura J, et al. HIF-1alpha is a crucial factor in the development of peritoneal dissemination via natural metastatic routes in scirrhous gastric cancer. *Int J Oncol.* 2013;43:1431–40.
24. Berx G, Van Roy F. The E-cadherin/catenin complex: an important gatekeeper in breast cancer tumorigenesis and malignant progression. *Breast Cancer Res.* 2001;3:289–93.
25. Paredes J, Figueiredo J, Albergaria A, et al. Epithelial E- and P-cadherins: role and clinical significance in cancer. *Biochim Biophys Acta.* 2012;1826:297–311.
26. Yin M, Ren X, Zhang X, et al. Selective killing of lung cancer cells by miRNA-506 molecule through inhibiting NF-kappaB p65 to evoke reactive oxygen species generation and p53 activation. *Oncogene.* 2014. doi: 10.1038/onc.2013.597.
27. Wen SY, Lin Y, Yu YQ, et al. miR-506 acts as a tumor suppressor by directly targeting the hedgehog pathway transcription factor Gli3 in human cervical cancer. *Oncogene.* 2014. doi:10.1038/onc.2014.9.
28. Liu G, Sun Y, Ji P, et al. MiR-506 suppresses proliferation and induces senescence by directly targeting the CDK4/6-FOXM1 axis in ovarian cancer. *J Pathol.* 2014;233:308–18.
29. Guo F, Parker Kerrigan BC, Yang D, et al. Posttranscriptional regulatory network of epithelial-to-mesenchymal and mesenchymal-to-epithelial transitions. *J Hematol Oncol.* 2014;7:19.
30. Liu Z, Chen L, Zhang X, et al. RUNX3 regulates vimentin expression via miR-30a during epithelial–mesenchymal transition in gastric cancer cells. *J Cell Mol Med.* 2014;18:610–23.
31. Maier HJ, Schmidt-Strassburger U, Huber MA, Wiedemann EM, Beug H, Wirth T. NF-kappaB promotes epithelial–mesenchymal transition, migration, and invasion of pancreatic carcinoma cells. *Cancer Lett.* 2010;295:214–28.
32. Takeshita F, Patrawala L, Osaki M, et al. Systemic delivery of synthetic microRNA-16 inhibits the growth of metastatic prostate tumors via downregulation of multiple cell-cycle genes. *Mol Ther.* 2010;18:181–7.
33. Lanford RE, Hildebrandt-Eriksen ES, Petri A, et al. Therapeutic silencing of microRNA-122 in primates with chronic hepatitis C virus infection. *Science.* 2010; 327:198–201.

Carcinogenesis vol.36 no.1 pp.133–141, 2015
doi:10.1093/carcin/bgu232
Advance Access publication November 19, 2014

Epigenetic modulation and repression of miR-200b by cancer-associated fibroblasts contribute to cancer invasion and peritoneal dissemination in gastric cancer

Junji Kurashige[1,2], Kosuke Mima[1,2], Genta Sawada[1,3], Yusuke Takahashi[1,3], Hidetoshi Eguchi[1], Keishi Sugimachi[1], Masaki Mori[3], Kazuyoshi Yanagihara[4], Masakazu Yashiro[5], Kosei Hirakawa[5], Hideo Baba[2] and Koshi Mimori[1,*]

[1]Department of Surgery, Kyushu University Beppu Hospital, 4546 Tsurumihara, Beppu, Oita 874-0838, Japan, [2]Department of Gastroenterological Surgery, Graduate School of Medical Sciences, Kumamoto University, 1-1-1 Honjo, Kumamoto, Kumamoto 860-8556, Japan, [3]Department of Gastroenterological Surgery, Osaka University Graduate School of Medicine, 2-2 Yamada-oka, Suita, Osaka 565-0871, Japan, [4]Division of Translational Research, Exploratory Oncology Research and Clinical Trial Center, National Cancer Center, 6-5-1, Kashiwanoha, Kashiwa, Chiba 277-8577, Japan and [5]Department of Surgical Oncology, Osaka City University Graduate School of Medicine, 1-4-3 Asahi-machi, Abeno-ku, Osaka 545-8585, Japan

*To whom correspondence should be addressed. Tel: +81-977-27-1650; Fax: +81-977-27-1651
Email: kmimori@beppu.kyushu-u.ac.jp

Cancer-associated fibroblasts (CAFs) have recently been linked to the invasion and metastasis of gastric cancer. In addition, the microRNA (miR)-200 family plays a central role in the regulation of the epithelial–mesenchymal transition process during cancer metastasis, and aberrant DNA methylation is one of the key mechanisms underlying regulation of the miR-200 family. In this study, we clarified whether epigenetic changes of miR-200b by CAFs stimulate cancer invasion and peritoneal dissemination in gastric cancer. We evaluated the relationship between miR-200b and CAFs using a coculture model. In addition, we established a peritoneal metastasis mouse model and investigated the expression and methylation status of miR-200b. We also investigated the expression and methylation status of miR-200b and CAFs expression in primary gastric cancer samples. CAFs (CAF-37 and CAF-50) contributed to epigenetic changes of miR-200b, reduced miR-200b expression and promoted tumor invasion and migration in NUGC3 and OCUM-2M cells in coculture. In the model mice, epigenetic changes of miR-200b were observed in the inoculated high-frequency peritoneal dissemination cells. In the 173 gastric cancer samples, the low miR-200b expression group demonstrated a significantly poorer prognosis compared with the high miR-200b expression group and was associated with peritoneal metastasis. In addition, downregulation of miR-200b in cancer cells was significantly correlated with alpha-smooth muscle actin expression. Our data provide evidence that CAFs reduce miR-200b expression and promote tumor invasion through epigenetic changes of miR-200b in gastric cancer. Thus, CAFs might be a therapeutic target for inhibition of gastric cancer.

Introduction

Scirrhous gastric cancer has a very poor prognosis due to its rapid infiltrative invasion and high incidence of peritoneal dissemination (1), and the 5-year survival rate of patients with peritoneal dissemination is only 2% (2). Thus, it is necessary to improve our understanding of the mechanisms involved in the spread of gastric cancer to the peritoneal cavity to identify novel therapeutic targets.

Abbreviations: CAF, cancer-associated fibroblast; EMT, epithelial–mesenchymal transition; FBS, fetal bovine serum; miRNA, microRNA; PBS, phosphate-buffered saline;RT–PCR, reverse transcription–PCR; SMA, smooth muscle actin; TGF, transforming growth factor.

Recent studies have established the importance of the tumor stroma in cancer progression and metastasis (3). Stromal fibroblasts are the major cellular constituents of tumor stroma, and are often referred to as cancer-associated fibroblasts (CAFs). They often display the phenotypes of myofibroblasts, which are characterized by the expression of α-smooth muscle actin (α-SMA) and strong contractility (4). Moreover, CAFs play an important role in the malignant progression of several cancers such as breast, prostate, pancreatic, esophageal and lung cancer, among others, including the initiation, proliferation, invasion and metastasis of cancer cells (5–7). A previous report indicated that gastric fibroblasts play an important role in the progression, growth and spread of scirrhous gastric cancers (8,9).

Recent evidence has emerged that directly or indirectly associates several microRNAs (miRNAs) with the epithelial–mesenchymal transition (EMT), contributing to the now extensive list of EMT-associated transcription factors (10,11). Gregory *et al.* and Park *et al.* demonstrated the clear involvement of the miR-200 family in this process, which consists of five members that can be divided into two clusters: miR-200a/b/429 and miR-200c/141, which map to human chromosomes 1 and 12, respectively (12). The miR-200 family has been suggested to play a central role in the regulation of the EMT process during cancer progression and metastasis. The most prominent gene targets of the miR-200 family are *ZEB1* and *ZEB2*, which are direct repressors of the EMT marker E-cadherin (13). We reported previously that miR-200b was an important regulator of EMT through inhibition of migration and invasion via targeting the mRNAs of *ZEB1* and *ZEB2* in gastric cancer cells (14). Several studies have shown that the miR-200 family inhibits translation of *ZEB1* and *ZEB2* mRNAs in several types of cancers (15–17). Moreover, in addition to the epigenetic regulation of *ZEB1* and *ZEB2* by miR200, previous reports have clarified that aberrant DNA methylation is observed in the promoter region of miR200 family themselves, which occurs subsequent to the induction of EMT by the reactivation of *ZEB1* and *ZEB2* in various cancers (18–20).

In the current study, we demonstrated that the epigenetic mechanisms involved in the regulation of the miR-200 family are not only restricted to malignant cells but are also apparent in CAFs. We found that miR-200b is epigenetically regulated and demonstrated a link between the epigenetics status of miR-200b and the presence of CAFs in gastric cancer cell lines, model mice and cancer tissue samples from patients. The purpose of this study was to evaluate how CAFs are involved in the progression and invasion of the corresponding adjacent cancer cells via epigenetic changes of miR-200b in gastric cancer.

Materials and methods

Cell lines and cell culture

Human gastric cancer cell lines (NUGC3, NUGC4, AGS, MKN1, MKN7, MKN28, MKN45 and AZ521) were obtained in 2012 from the Cell Resource Center for Biomedical Research Institute of Development, Aging and Cancer, Tohoku University, Japan. Human gastric cancer cell lines (OCUM-2M and OCUM-2MD3) and human gastric fibroblast cell lines (CAF-37 and CAF-50) were obtained from gastric carcinoma population maintained at Osaka City University (21,22). The fibroblasts were used in the 3rd through 12th passage in culture and mainly at the 5th passage. To examine the incubating myofibroblast content of orthotopic fibroblasts, immunohistochemical staining was performed as described previously (9). HSC-58 cells were established previously from a patient with scirrhous gastric cancer. HSC-58 cells inoculated into BALB/c nude mice led to dissemination of the tumor cells to the greater omentum, mesenterium, peritoneum and so on and caused ascites in a small number of animals. Cycles of isolation and orthotopic inoculation of the ascitic tumor cells were repeated in the mice for a total of 12 cycles. We obtained two cell lines (58As1Luc and 58As9) that possessed high metastatic potential and showed strong capability of inducing ascites (23). HSC-58, 58As1Luc and 58As9

have no KRAS mutation. NUGC3, NUGC4, AGS, MKN1, MKN7, MKN28, MKN45, AZ521, HSC-58, 58As1Luc and 58As9 cells were cultured in RPMI 1640 with 10% fetal bovine serum (FBS; Life Technologies, Grand Island, NY) with 100 IU/ml penicillin and 100 mg/ml streptomycin. OCUM-2M, OCUM-2MD3, CAF-37 and CAF-50 cells were cultured in Dulbecco's modified Eagle's medium (Nikken, Kyoto, Japan) with the addition of 10% heat-inactivated FBS, 100 IU/ml penicillin, 100 mg/ml streptomycin and 0.5 mM sodium pyruvate. Cells were cocultured in Transwell chambers separated by 8 μm pore filters. Gastric cancer cells (3.0×10^5 cells/700 μl) were placed in the bottom chamber, and CAF-37 and CAF-50 (2.0×10^4 cells/300 μl) were placed in the top chamber. After 5 days, the top chamber was removed, and RNA was isolated from cancer cells. NUGC3, OCUM2M, AZ521, HSC-58, 58As1Luc and 58As9 were authenticated by short tandem repeat–PCR analysis. DNA was extracted by each cell line with QIAamp DNA Mini Kit (QIAGEN) and characterized by short tandem repeat–PCR analysis using GenePrint® 10 System (Promega).

Clinical samples

Primary gastric carcinoma tissue and matched normal gastric epithelium samples were obtained from 173 patients who underwent gastric resection without preoperative treatment at Oita Prefectural Hospital, Kyushu University Beppu Hospital between 1993 and 2003. All tissue samples were immediately cut from gastric resections, placed in RNA Later (Takara, Japan), frozen in liquid nitrogen and stored at −80°C until RNA extraction. Moreover, 53 formalin-fixed, paraffin-embedded gastric cancer tissues from Kyushu University Beppu Hospital were used in this study. Written informed consent was obtained from all patients, and the study protocol was approved by the local ethics committee. Clinicopathological information, including age, gender, pathology, differentiation and tumor-node-metastasis classification, was available for all patients.

Total RNA isolation and first-strand complementary DNA synthesis

Total RNA was isolated from frozen tissue samples by means of the modified acid-guanidine-phenol-chloroform method and isolated from cultured cell lines by using the miRNeasy Mini Kit (QIAGEN), as described previously (24,25). The purity and concentration of all RNA samples were evaluated by the absorbance ratio at 260/280 nm with a NanoDrop ND-1000 spectrophotometer (NanoDrop Technologies, Rockland, DE). Total RNA was reverse transcribed to complementary DNA with M-MLV RT (Invitrogen, Carlsbad, CA).

Quantitative real-time reverse transcription–PCR

The expression of miR-200a, b, miR-429 was determined by TaqMan quantitative real-time reverse transcription–PCR (qRT–PCR) using TaqMan microRNA assay kits (Ambion) according to the manufacturer's protocols, as described previously (14). miR-200a, b, miR-429 expression was normalized to that of the small nuclear RNA *RNU6B*. The expression of *CDH1*, *ZEB1*, *ZEB2* and *Vimentin* was determined using a LightCycler 480 probes master kit (Roche Diagnostics,) according to the manufacturer's instructions. Primers and TaqMan assays are listed in Supplementary Table 1, available at *Carcinogenesis* Online. All qRT–PCRs were run in a LightCycler 480 System II (Roche Diagnostics; USA). The relative amounts of miR-200a, b, miR-429, *CDH1*, *ZEB1*, *ZEB2* and *Vimentin* were measured using the $2^{-\Delta\Delta CT}$ method. All qRT–PCRs were performed in triplicate.

miRNA microarray of HSC-58, 58As1Luc and 58As9

RNA was extracted from each cell line, and RNA samples were dephosphorylated and labeled with Cyanine 3-pCp using T4 RNA ligase by incubating at 16°C for 2 h. After the labeling reaction, the samples were completely dried using a vacuum concentrator at 55°C for 4 h. The dried samples were treated with GE blocking agent. The SurePrint G3 Human v16 miRNA 8×60 K array, which contains probes for 1205 human and 144 human viral miRNAs, was used for miRNA profiling. The blocked samples were hybridized to the probes on the microarray at 55°C with constant rotation at 20 r.p.m. in the Agilent microarray hybridization chamber for 20 h. The microarray slide was washed and scanned using the Agilent scanner to obtain the microarray image. The numerical data for the miRNA profiles were extracted from the image using the Feature Extraction program. These data were analyzed with the aid of GeneSpring GX software, version 7.3 (all from Agilent Technologies). We normalized the observed expression levels of miRNA through the procedure of quantile normalization, and miRNAs displaying an increase or decrease >2-fold were selected for further analysis. MiRNAs that displayed increased and decreased expression are listed in Supplementary Table 2, available at *Carcinogenesis* Online, and Table I, respectively.

DNA methylation analysis and 5-aza-2′-deoxycytidine treatment

CpG islands were identified *in silico* using Methyl Primer Express v1.0 software (Applied Biosystems, Carlsbad, CA). DNA methylation status was established by bisulfite genomic sequencing of multiple clones and methylation-specific PCR. The primer sequences used in the DNA methylation analysis are listed in Supplementary Table 1, available at *Carcinogenesis* Online. Cells were treated with 2.5 or 5.0 μM 5-aza-2′-deoxycytidine (5-aza-dC; Sigma–Aldrich, St Louis, MO) for 48 h.

Table I. Summary of significantly differentially expressed miRNAs in 59As1Luc and 59As9 cells compared with HSC-59 cells

Rank	microRNA	Chromosomal location	Fold change(log2)
Decreased expression in 59As1Luc compared with HSC-58			
1	hsa-miR-31-3p	9p21	−8.42
2	hsa-miR-141-3p	12p13	−8.32
3	hsa-miR-200a-3p	1p36	−5.62
4	hsa-miR-135b-5p	1q32	−5.47
5	hsa-let-7g-5p	3p21	−5.35
6	hsa-miR-98-5p	Xp11	−5.34
7	hsa-miR-532-5p	Xp11	−5.30
8	hsa-miR-27b-3p	9q22	−5.25
9	hsa-miR-10b-5p	2q31	−5.20
10	hsa-let-7d-5p	9q22	−5.19
11	hsa-miR-10a-5p	2q31	−5.06
12	hsa-let-7f-5p	17q21	−4.93
13	hsa-miR-27a-3p	19p13	−4.92
14	hsa-miR-28-5p	3q28	−4.84
15	hsa-miR-23b-3p	9q22	−4.79
16	hsa-miR-192-3p	11q13	−4.74
17	hsa-miR-4284	7q11	−4.67
18	hsa-miR-200b-3p	1p36	−4.45
Decreased expression in 59As9 compared with HSC-58			
1	hsa-miR-141-3p	12p13	−8.84
2	hsa-miR-548ag	4q13	−6.70
3	hsa-miR-4510	15q14	−4.04
4	hsa-miR-520g	19q13	−3.22
5	hsa-miR-130a-3p	11q12	−2.82
6	hsa-miR-520d-3p	19q13	−2.70
7	hsa-miR-338-3p	17q25	−2.67
8	hsa-miR-429	1p36	−2.65
9	hsa-miR-200a-3p	1p36	−2.58
10	hsa-miR-548ai	6q16	−2.45
11	hsa-miR-374a-3p	Xq13	−2.39
12	hsa-miR-520b	19q13	−2.33
13	hsa-miR-135b-5p	1q32	−2.28
14	hsa-miR-200b-3p	1p36	−2.26

Migration and invasion assays

Cell migration and invasion were assessed using the BD Falcon FluoroBlok™ 24 Multiwell Insert System (BD Bioscience, San Jose, CA) using 8 mm pore-sized membranes with Matrigel (for invasion assays) or without Matrigel (for migration assays). In brief, 2×10^4 CAF-37 and CAF-50 cells were placed in 750 μl of medium containing 10% FBS in the lower chamber. The medium containing 10% FBS but no cells were added to the lower chamber of control wells. The NUGC3 cells (1×10^5) were placed in the upper chamber of a 24-well plate with serum-free medium. The cell plate was incubated in a humidified atmosphere (37°C and 5% CO_2). After 48 h incubation, the upper chamber was transferred to a second 24-well plate containing 500 μl/well of 4 μg/ml calcein AM in Hanks' balanced salt solution and incubated for 1 h (37°C and 5% CO_2). Invasive cells that migrated through the membrane were evaluated in a fluorescence plate reader at excitation/emission wavelengths of 485/535 nm. Each independent experiment was performed three times.

Immunohistochemistry and quantitative analysis of α-SMA.

Immunohistochemical studies of α-SMA were performed on formalin-fixed, paraffin-embedded surgical sections obtained from patients with gastric cancer. Tissue sections were deparaffinized and boiled in 0.01 mol/l sodium citrate buffer in a microwave for 10 min at 500 W for antigen retrieval. Rabbit anti-α-SMA (ab5694; Abcam, Cambridge, UK), diluted 1:100, was used as the primary antibody. All tissue sections were immunohistochemically stained with the avidin-biotin-peroxidase method (LSAB System HRP; Dako, Kyoto, Japan) and were counterstained with hematoxylin. α-SMA expression in cancer-associated stroma was quantified as the relative percentage of the α-SMA-stained area to the selected field area using an imaging processor, as described previously (26,27). Slides were observed under light microscopy at ×100 magnification, and five regions were selected for every slide at random. The expression was independently evaluated by two of the authors (J.K. and K.M.)

using a blinded protocol design (the observers had no information on clinical outcome or any other clinicopathological data). ImageJ software was used to analyze the positive area percentage and staining intensity in the stroma tissue of every region, and then the average value was calculated from the amount of α-SMA on every slide (Supplementary Figure 1, available at *Carcinogenesis* Online). The muscle layer region was avoided for this assessment because muscle fibers ubiquitously express α-SMA.

Immunoblotting for E-cadherin

For immunoblotting, sodium dodecyl sulfate–polyacrylamide gel electrophoresis of proteins was performed using NuPAGE 4–12% Bis-Tris Gel electrophoresis (Invitrogen), an XCell Sure Lock Mini-cell (Invitrogen), and a Power PAC HC (Bio-Rad). The resolved proteins on the gel were transferred to a nitrocellulose membrane using iBlot Dry Blotting System (Invitrogen). The resulting membranes were blocked with 5% iBlot (Applied Biosystems) and 0.1% Tween-20 (Bio-Rad) in phosphate-buffered saline (PBS) (T-PBS) for 1 h. Membranes were then incubated with primary antibodies. Next, the membranes were washed twice for 5 min in T-PBS, incubated with an horseradish peroxidase-conjugated secondary antibody for 1 h and washed twice for 5 min in T-PBS.

Chemiluminescence detection reagents were incubated with the membranes for 1–5 min, followed by image acquisition using an Image Quant LAS500 (GE Healthcare). Primary antibodies targeted pan actin (NeoMarkers) and a monoclonal antibody against E-cadherin (1:200, BD Bioscience) diluted 1:200.

Orthotropic in vivo *models*

Six-week-old female BALB/c nu/nu mice were purchased from Kyudo Japan and maintained under specific pathogen-free conditions and provided with sterile food, water and cages. Ambient light was controlled to provide regular cycles of 12 h of light and 12 h of darkness. A total of 1×10^6 HSC-58, 58As1Luc and 58As9 cells were inoculated into the gastric wall of each mouse after laparotomy, as described previously (23,28,29). For, assessment of miR-200b influence, a total of 1×10^6 cancer cells [58As9 with Pre-miR™ miRNA Precursor Molecule Negative Control and Pre-miR™ miRNA Precursor Molecule pre-200b (Applied Biosystems, Foster City, CA)] were inoculated into the gastric wall of each mouse. The method of transfection of miRNA was following the past manuscript (14). At 28 days after inoculation, the mice were sacrificed and dissected and peritoneal dissemination, liver metastasis and ascites formation were examined. The number of mesentery nodules >5 mm in diameter was also determined. All animal procedures were performed in compliance with the Guidelines for the Care and Use of Experimental Animals established by the Committee for Animal Experimentation of Kyushu University; these guidelines conform to the ethical standards required by Japanese law and also comply with the guidelines for the use of experimental animals in Japan.

Statistical analysis

All experiments were performed at least three times. Continuous variables are expressed as the means ± standard deviations. The relationship between the expression of miR-200b and the patient clinicopathological characteristics was analyzed using the Student's *t*-test or a chi-square analysis. The overall survival curves were plotted according to the Kaplan–Meier method, and the generalized log-rank test was applied to compare the survival curves. The findings were considered to be significant for *P*-values < 0.05. All tests were performed using JMP software, eighth edition (SAS Institute, Cary, NC).

Results

CAFs stimulated the invasion and migration of gastric cancer via epigenetic change of the miR-200b promoter

We used the coculture system to determine whether CAFs secrete factors that could stimulate the invasion and migration of gastric cancer cells *in vitro*. NUGC3 cells treated with CAFs (CAF-37 and CAF-50) showed significantly high migratory behavior ($P < 0.01$; Figure 1A, left) and were significantly invasive ($P < 0.01$; Figure 1A, right) compared with NUGC3 cells only (NUGC3 control). We examined miR-b expression in the gastric cancer cell lines cocultured with CAFs. The miR-200b expression in NUGC3 and OCUM-2M cells (which showed high miR-200b expression and low methylation) treated with CAFs was lower than those of control cells ($P < 0.05$; Figure 1B). Similarly, the levels of *CDH1* mRNA and protein, an EMT marker, of NUGC3 and OCUM-2M cells treated with CAFs were lower than those of control cells (Figure 1C and E). Recent evidence suggests that expression of miR-200 family members can be epigenetically regulated through methylation of their promoter regions (18,19,30). Therefore, we evaluated the methylation status to identify the mechanism of downregulation of miR-200b by CAFs in gastric cancer. The miR-200b/200a/429 transcription start sites have been determined previously to be located within canonical CpG islands in chromosome 1 (31,32). The CpG islands of the miR-200b promoter in gastric cancer cells treated with CAFs showed an increased amount of partially methylated changes than those of control cell lines (Figure 1D). Moreover, we examined miR-200a and 429 expression in the gastric cancer cell lines cocultured with CAFs. Similarly to miR-200b, the expression of both miR-200a and 429 in NUGC3 cells treated with CAFs were lower than those of control cells (Supplementary Figure 2, available at *Carcinogenesis* Online).

CpG island hypermethylation-associated silencing of miR-200b in cancer cells

miR-200b is suggested to target *ZEB1/2*, thereby preventing the repression of E-cadherin expression by *ZEB1/2*. We evaluated the correlation between miR-200b and *CDH1*, *Vimentin* and *ZEB1/2* mRNA expression in 14 gastric cancer cell lines. As shown in Supplementary Figure 3A–E, available at *Carcinogenesis* Online, the high miR-200b expression cell lines, OCUM-2M, MKN45, KATOIII and OCUM-8, showed low *ZEB1*, *ZEB2* and *Vimentin* expression, whereas the low miR-200b expression cell lines, AZ521 and MKN1, showed high *ZEB1*, *ZEB2* and *Vimentin* expression and low *CDH1* expression. The CpG islands of the miR-200b/200a/429 cluster were almost completely methylated in AZ521 cells, which showed the lowest miR-200b expression, whereas OCUM-2M and NUGC31 cells, which showed high miR-200b expression, were found to be almost completely unmethylated (Supplementary Figure 3F, available at *Carcinogenesis* Online). To further understand the functional significance of promoter hypermethylation of miR-200b, we treated AZ521 cells with the DNA-demethylating agent 5-aza-2′-deoxycytidine. Indeed, treatment of AZ521 with 5-aza-2′-deoxycytidine restored the expression of miR-200b (Supplementary Figure 3G, available at *Carcinogenesis* Online)

The epigenetic change of miR-200b in scirrhous cancer with high peritoneal dissemination

Two highly metastatic cell lines (58As1Luc and 58As9) were also established from the HSC-58 cells. When 58As1Luc or 58As9 cells were implanted orthotopically, bloody ascites began to form ~3 weeks after the inoculation, accompanied by tumor dissemination to the greater omentum, mesenterium, parietal peritoneum, diaphragm and so on, and the mice died soon thereafter (Figure 2A and B). We performed miRNA microarray profiling between HSC-58, 58As1Luc and 58As9 cells. As a result, the miR-200 family was significantly downregulated in 58As1Luc and 58As9 cells compared with HSC-58 cells (Table I). We next performed quantitative RT–PCR to confirm the microarray results. Similarly, miR-200b expression was downregulated in 58As1Luc and 58As9 cells compared with HSC-58 cells (Figure 2C). The CpG islands were partially methylated in 58As1Luc and 58As9 cells, which showed low miR-200b expression; in contrast, CpG islands of HSC-58 cells, which showed high miR-200b expression, were methylated at a much lower frequency (Figure 2D). Treatment with 5-aza-2′-deoxycytidine in 58As1Luc and 58As9 cells restored the expression of miR-200b (Figure 2E). Next, we orthotropically inoculated 58As9 with miR-200b upregulated in the stomach wall of nude mice. After twenty-eight days of orthotropic transplantation, we confirmed miR-200b upregulated markedly were showed that reduction number of disseminated metastasis (Figure 2F).

Association of miR-200b expression with clinicopathological characteristics and survival

Expression of miR-200b was examined in 173 clinical gastric cancer samples using qRT–PCR, with quantified values used to calculate miR-200b/RNU6B ratios. The mean expression of miR-200b

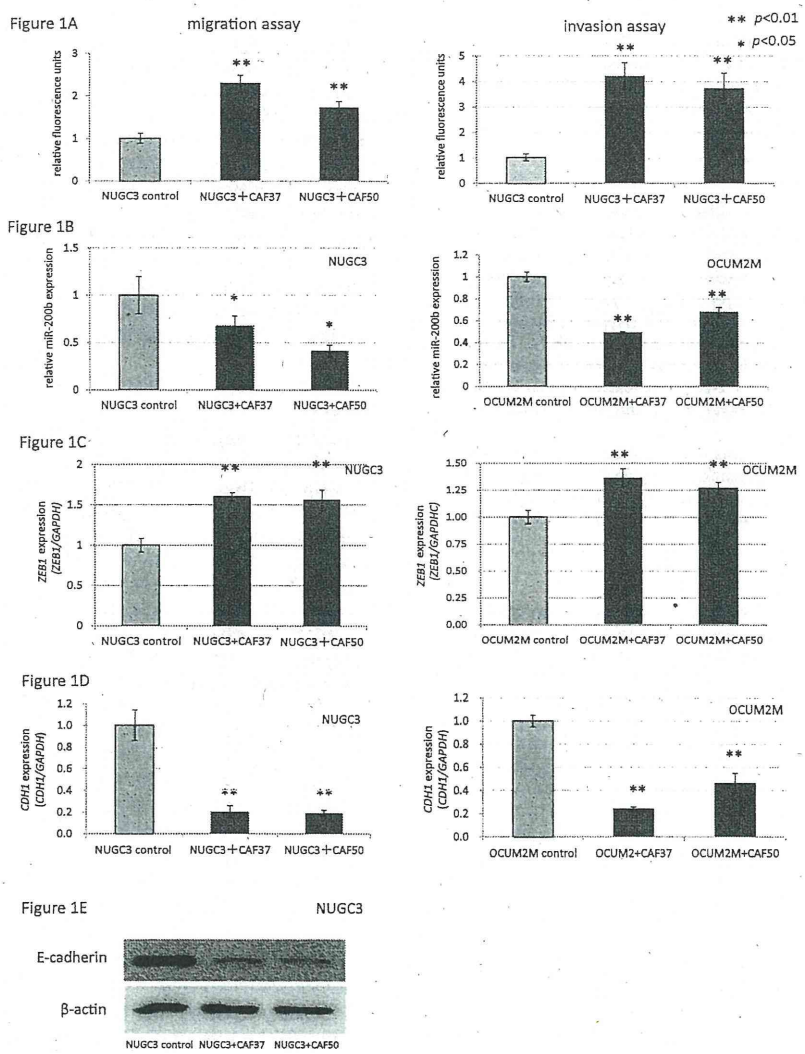

Fig. 1. CAFs stimulated the invasion and migration of gastric cancer via epigenetic changes of the miR-200b promoter. (**A**) NUGC3 cells treated with CAF-37 and CAF-50 showed significantly high migratory and invasive behavior compared with NUGC3 control cells. (**B**) The expression of miR-200b, (**C**) *ZEB1* and (**D**) *CDH1* expression in NUGC3 and OCUM-2M cancer cells in the coculture model. (**E**) The CpG islands of miR-200b in gastric cancer cells showed increased partial methylation in the coculture model. (**F**) E-cadherin expression in NUGC3 and OCUM-2M cancer cells was significantly downregulated in the coculture model.

in cancerous tissue specimens was significantly lower than those in non-cancerous tissues ($P < 0.01$; Figure 3A). Moreover, the mean expression of miR-200b in the cancerous tissue specimens of patients with peritoneal metastasis was significantly lower than those without peritoneal metastasis (peritoneal metastasis included cytology-positive samples; $P < 0.01$; Figure 3B). We divided the 173 gastric cancer patients into two groups according to the median miR-200b expression level: 87 of the cases were placed in the high miR-200b expression group and the remaining 86 cases were placed in the low miR-200b expression group. The association between patient clinicopathological characteristics and miR-200b expression is summarized in Table II. miR-200b expression was significantly associated with cancer differentiation (well and moderately differentiated versus poorly differentiated and others; $P = 0.002$), depth of tumor invasion (T1 and T2 versus T3 and T4; $P = 0.010$), venous invasion (present versus absent; $P = 0.017$), peritoneal metastasis (present versus absent; $P < 0.001$), distant metastasis (including peritoneal metastasis, present versus absent; $P = 0.002$) and cancer staging (stage I and II versus stage III and IV; $P = 0.005$). Analysis of 5-year overall survival showed that the low miR-200b expression group had significantly poorer prognosis than the high expression group ($P = 0.015$; Figure 3C).

Expression of CAFs in gastric cancer stroma and association with miR-200b in gastric cancer specimens

Next, we verified the relationship between the epigenetic status of miR-200b and CAFs surrounding cancer cells in clinical gastric cancer samples. Stromal fibroblasts in 53 gastric cancer samples were quantified using a computer-assisted image analysis system as described in the Materials and methods. A representative photograph stained for α-SMA and the corresponding image treated with an imaging processor are shown in Supplementary Figure 1A–F, available at *Carcinogenesis* Online. The α-SMA staining localized in the cytoplasm of stroma fibroblasts, whereas tumor cells were negatively stained. The α-SMA scores varied from 0.31 to 9.47% (mean, 3.59%). Two investigators (J.K. and K.M.) independently evaluated α-SMA staining and obtained similar results. Next, we examined the correlation between α-SMA staining in gastric cancer stroma

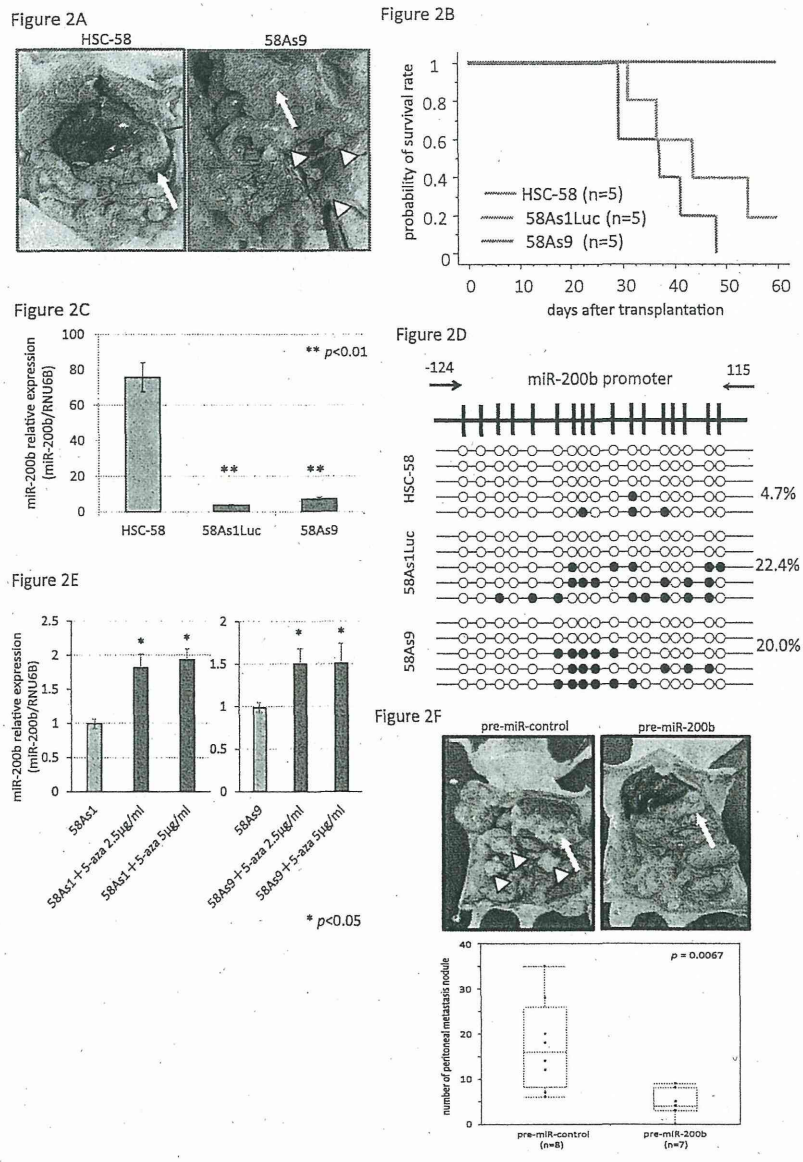

Fig. 2. Silencing miR-200b by epigenetic changes in model mice of scirrhous cancer with high frequency of peritoneal dissemination. (**A** and **B**) 58As9 cells were implanted orthotopically, and bloody ascites began to form ~3 weeks after the inoculation, accompanied by tumor dissemination to the peritoneum; mice with implanted 58As9 cells died faster than mice with implanted HSC-58 cells. White arrows: orthotopic implantation of the cells in the stomach wall of nude mice led to tumor formation within 3 weeks. Blue arrows:, nodules visualized in the abdominal cavity, mesenterium. (**C**) The miR-200b expression in 58As1Luc and 58As9 cells was downregulated compared with HSC-58 cells, as determined by quantitative RT–PCR. (**D**) Whereas HSC-58 cells were found to be unmethylated, the CpG islands of miR-200b promoter regions were partially methylated in 58As1Luc and 58As9 cells. (**E**) Treatment with 5-aza-2′-deoxycytidine in 58As1Luc and 58As9 cells restored the expression of miR-200b. (**F**) Number of disseminated metastasis tumor after 28 days inoculation of 58As9 with miR-200b upregulated. Control, pre-miR-200b are each $n = 8$ and 7.

and miR-200b expression in gastric cancer. There was a significant inverse correlation between miR-200b expression and the α-SMA score (Figure 4A). The gastric cancer samples were then divided into two groups, a high α-SMA group ($n = 26$) and a low α-SMA group ($n = 27$), according to α-SMA expression in stroma at a cut-off point at the median mean value. The patients with high α-SMA expression had significantly lower miR-200b expression than the low α-SMA patients ($P < 0.05$; Figure 4B). When α-SMA expression was compared with the various clinical and pathologic variables listed in Supplementary Table 3, available at *Carcinogenesis* Online, no significant associations were found. Moreover, we chose three low miR-200b/high α-SMA scoring patients and three high miR-200b/low α-SMA scoring patients for further analysis (Supplementary Figure 4, available at *Carcinogenesis* Online). The CpG islands were more significantly methylated in the low miR-200b/high α-SMA group than in the high miR-200b/low α-SMA group (Figure 4C).

Discussion

In this study, we demonstrated that CAFs reduced miR-200b expression and induced the hypermethylation of the miR-200b promoter regions. Furthermore, there was a negative correlation between miR-200b expression in gastric cancer specimens and α-SMA

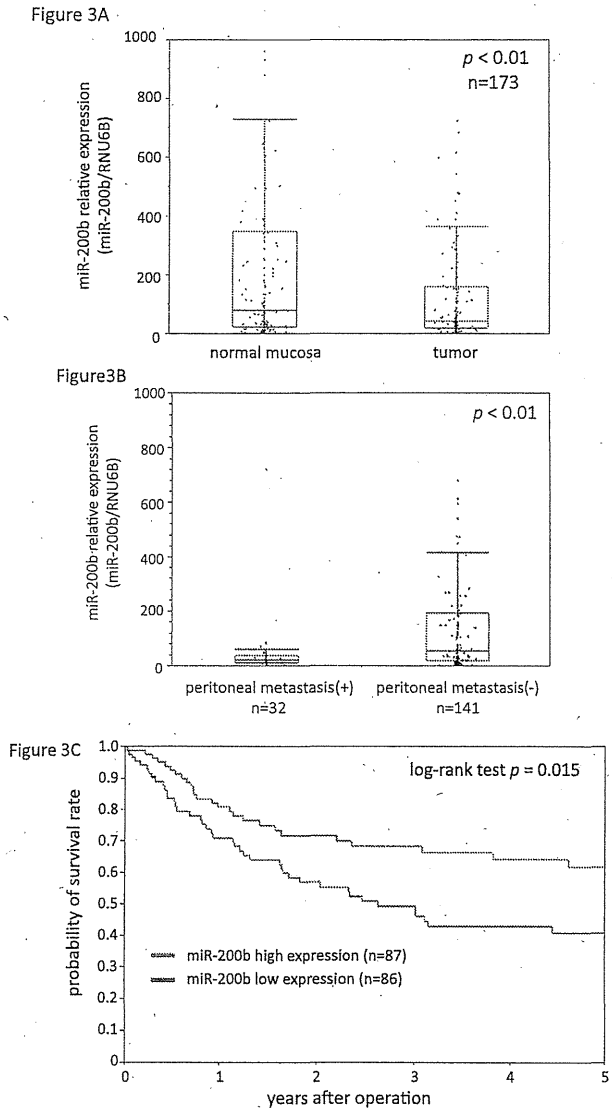

Fig. 3. Expression status of miR-200b and Kaplan–Meier survival curves in gastric cancer patients. (**A**) The mean expression levels of miR-200b in cancerous tissue specimens were significantly lower than those in non-cancerous tissues ($P < 0.01$). (**B**) The mean expression levels of miR-200b in the cancerous tissue specimens of patients with peritoneal metastasis ($n = 32$) were significantly lower than those without peritoneal metastasis ($n = 141$) ($P < 0.01$). (**C**) The overall survival curves are presented according to the expression level of miR-200b in gastric cancer patients. Patients with low miR-200b expression ($n = 86$) had a poorer prognosis than those with high expression ($n = 87$) (log-rank test; $P = 0.015$).

expression in the stroma of gastric cancer, and the patients with high α-SMA expression showed methylation of the miR-200b promoter. These findings suggest that CAFs stimulate cancer invasion and migration via epigenetic changes of miR-200b in gastric cancer. Moreover, model mice with peritoneal dissemination showed methylated miR-200b and low miR-200b expression. Similarly, we found that patients with low miR-200b expression had a significantly poorer prognosis than those with high miR-200b expression, and low miR-200b expression was associated with peritoneal dissemination.

This is the first study to directly analyze the role of CAFs to regulate the expression of miRNA via epigenetic changes to the best of our knowledge. The CAFs populations in tumor-associated stroma are known to include both fibroblasts and myofibroblasts. Myofibroblasts are endowed with the ability to promote tumor growth and are associated with higher grade malignancy and poorer prognosis in patients with several cancers (26,33,34). Indeed, the CAFs prepared and examined in our study contained a subpopulation of α-SMA-expressing fibroblasts, as indicated by immunohistochemistry (Figure 4 and Supplementary Figure 2, available at *Carcinogenesis* Online). CAFs can promote cancer progression, invasion and metastasis by modulating multiple components in the cancer niche to build a permissive and supportive microenvironment for tumor growth and invasion through the secretion of growth factors including hepatocyte growth factor, stromal cell-derived factor-1, several chemokine factors, platelet-derived growth factor, fibroblast growth factor and transforming growth factor (TGF)-β (35–38). In particular, TGF-β from tumor-associated stroma is an important factor for the induction and functional activation of EMT-related pathways (39–41). Interestingly, TGF-β was shown to induce the expression of DNA methyltransferases, which function in DNA methylation, in several cancers (42–44). Moreover, TGF-β also mediates these effects through the action of epigenetic switches such as CD133 and tristetrapolin, as well as miR-200 CpG island methylation events (18,42,45). Thus, in this study, some signals from CAFs, such as TGF-β, might be related to the corresponding methylation changes observed in miR-200b. This aspect remains to be investigated in future research.

Members of the miR-200 family are being increasingly recognized as important players for regulating epithelial characteristics of cells through direct targeting of *ZEB1* and *ZEB2*, which are EMT-inducing transcription factors, via transcriptional repression of E-cadherin expression (13,46); our present results in gastric cancer cell lines confirm this role of miR-200 (Supplementary Figure 2A–E, available at *Carcinogenesis* Online). Based on the EMT hypothesis of cancer metastasis, low expression of the miR-200 family would lead to increased metastasis through the targeted induction of *ZEB1* and *ZEB2* expression, resulting in repressed E-cadherin expression and the adoption of mesenchymal characteristics. This EMT process has been shown to occur in several types of cancer cells, whereby lower levels of the miR-200 family have been associated with a higher frequency of invasive and metastatic tumors and a poorer prognosis (16,46–48). However, several studies have also shown the opposite effect of high expression of miR-200 family members enhancing distant metastases through promoting secondary cancer colonization (30,49,50) in the mesenchymal–epithelial transition process. This has been interpreted as a potential requirement for EMT to accomplish the first steps of metastasis, and a reversion (mesenchymal–epithelial transition) to accomplish the final step of colonization. EMT is first acquired in the onset of transmigration and then reversed mesenchymal–epithelial transition occurs in the new colony; this process is described as epithelial–mesenchymal plasticity. However, because peritoneal dissemination is the most common cause of death in gastric cancer, a better understanding of the EMT mechanism is critical for developing new treatments that can improve the survival of gastric cancer patients with peritoneal dissemination. During EMT, methylation-induced downregulation of miR-200b allows upregulation of several of its direct target genes, including *ZEB1* and *ZEB2*, as they increase invasive and metastatic potential, involving the simultaneous loss of E-cadherin and enhancement of Vimentin expression at peritoneal dissemination sites. Our results demonstrated that restoration of miR-200b expression is a potential candidate approach for miRNA-based therapy against peritoneal dissemination of gastric cancer.

In conclusion, this study provides important insight supporting the roles of miR-200b during peritoneal dissemination in gastric cancer. Our discovery of the pivotal role that miR-200b plays in the metastatic behavior of gastric cancer indicates that this miRNA has potential value as a diagnostic and prognostic biomarker. These results may also have implications for the clinical management of patients with peritoneal dissemination.